AD-769 098

VOLUME HOLOGRAPHIC MATERIAL DEVICE FEASIBILITY FOR MAP DISPLAY APPLICATIONS

RCA Laboratories

PREPARED FOR
Naval Air Development Center

June 1973

AD-769098

UNCLASSIFIED
Security Classification

DOCUMENT CONTROL DATA - R & D
(Security classification of title, body of abstract and indexing annotation must be entered when the overall report is classified)

1. ORIGINATING ACTIVITY (Corporate author)
RCA Laboratories
Princeton, NJ 08540

2a. REPORT SECURITY CLASSIFICATION
Unclassified

2b. GROUP
N/A

3. REPORT TITLE
VOLUME HOLOGRAPHIC MATERIAL DEVICE FEASIBILITY FOR MAP DISPLAY APPLICATIONS

4. DESCRIPTIVE NOTES (Type of report and inclusive dates)
Final Report (18 May 1972 to 17 May 1973)

5. AUTHOR(S) (First name, middle initial, last name)
William J. Burke and David L. Staebler

6. REPORT DATE	7a. TOTAL NO. OF PAGES	7b. NO. OF REFS
June 1973	59	22

8a. CONTRACT OR GRANT NO.	9a. ORIGINATOR'S REPORT NUMBER(S)
N62269-72-C-0793	PRRL-73-CR-34
b. PROJECT NO.	
c.	9b. OTHER REPORT NO(S) (Any other numbers that may be assigned this report)
d.	

10. DISTRIBUTION STATEMENT
Approved for Public Release; Distribution Unlimited.

11. SUPPLEMENTARY NOTES	12. SPONSORING MILITARY ACTIVITY
	Department of the Navy Naval Air Development Center Warminster, PA

13. ABSTRACT

This report describes the results of a program to apply recent advances in the area of volume phase holographic materials for map storage and display applications, and to develop and evaluate subsystem components and techniques for this purpose. The major achievement of this program was the recording and fixing of up to 100 holograms in a given volume using a new technique for fixing in heavily iron-doped $LiNbO_3$. In addition, a mechanical random-access system for retrieving up to 100 holograms was developed and tested. An investigation was made of direct and indirect display formats, including incoherent readout of thick phase holograms and the recording and playback of encoded object transparencies on a color kinescope. This led to the conclusions that electronic pickup of the readout image is required for maximum utilization of the potential of a volume holographic storage system.

DD FORM 1 NOV 68 1473

UNCLASSIFIED
Security Classification

14 KEY WORDS	LINK A		LINK B		LINK C	
	ROLE	WT	ROLE	WT	ROLE	WT
Charge transport						
Conductivity						
Holographic fixing						
Holographic storage						
Holography						
Lithium niobate						
Photochromism						
Reduction treatments						

VOLUME HOLOGRAPHIC MATERIAL DEVICE FEASIBILITY FOR MAP DISPLAY APPLICATIONS

FINAL REPORT

BY

W. J. BURKE AND D. L. STAEBLER

PREPARED UNDER
CONTRACT NO. N62269-72-C-0793

JUNE 1973

FOR
DEPARTMENT OF THE NAVY
NAVAL AIR DEVELOPMENT CENTER
WARMINSTER, PA

BY
RCA LABORATORIES
PRINCETON, NJ 08540

FOREWORD

The research reported in this Final Report was performed in the Physical Electronics Laboratory of RCA Laboratories under Contract No. N62269-72-C-0793. G. D. Cody is the Laboratory Director and W. J. Burke is the Project Scientist. D. L. Staebler contributed significantly to the research and to this report. Other members of the Technical Staff who participated in the research are J. J. Amodei and R. A. Bartolini.

The program was sponsored by the Naval Air Systems Command, Washington, DC, under the direction of J. Wolin and R. Berthot. The contract was administered by the Naval Air Development Center, Warminster, PA, with K. W. Priest and K. D. Quiring as technical monitors.

ABSTRACT

This report describes the results of a program to apply recent advances in the area of volume phase holographic materials for map storage and display applications, and to develop and evaluate subsystem components and techniques for this purpose. The major achievement of this program was the recording and fixing of up to 100 holograms in a given volume using a new technique for fixing in heavily iron-doped $LiNbO_3$. In addition, a mechanical random-access system for retrieving up to 100 holograms was developed and tested. An investigation was made of direct and indirect display formats, including incoherent readout of thick phase holograms and the recording and playback of encoded object transparencies on a color kinescope. This led to the conclusion that electronic pickup of the readout image is required for maximum utilization of the potential of a volume holographic storage system.

TABLE OF CONTENTS

TABLE OF CONTENTS (Continued)

LIST OF ILLUSTRATIONS

LIST OF ILLUSTRATIONS (Continued)

I. INTRODUCTION

Volume holography has long been recognized as an attractive approach to the problem of optical storage of information. The reasons for this interest lie in the potential for truly high-density storage and in the simple methods required for hologram retrieval. The advantage over planar storage media lies in the extra dimension (i.e., the thickness) of the medium. The individual holograms are accessed by changing the angle of incidence of the light beam on the storage medium. Practical implementation had not been achieved in the past because storage media with the required high writing sensitivity, large multiple storage capacity, and resistance of the holograms to erasure by the readout light did not exist.

In a previous phase of this program, $LiNbO_3$ was found to possess all of the properties desired for volume storage. An intensive materials effort has led to significant improvement in the sensitivity and multiple storage capacity, and to the development of fixing techniques for holograms stored in $LiNbO_3$. These results have made $LiNbO_3$ the leading candidate for a volume holographic storage medium.

The current phase of this program has as its purposes the investigation of the applicability of $LiNbO_3$ to a volume holographic storage system for a moving map display and the assessment of the feasibility of such a system and its components. In this report we shall discuss the results of the recording and fixing of up to 100 holograms in Fe-doped $LiNbO_3$, the development and testing of a random-access retrieval system, and the testing and evaluation of several different output display formats.

II. STORAGE MATERIAL

The recording medium was Fe-doped $LiNbO_3$, an impurity-doped electro-optic single-crystal material. This material appears to be the most promising candidate for volume holographic map storage, primarily because of recent improvements in multiple storage and fixing. The techniques and mechanisms of storage and fixing are discussed here. In Section III we describe the problems associated with storage of many holograms within a crystal of Fe-doped $LiNbO_3$.

A. HOLOGRAM STORAGE

Holograms are recorded in electro-optic materials by generation of space charge patterns that modulate the refractive index via the electro-optic effect[1]. For this to occur, the material must contain a set of electron traps that can be photo-ionized by light. In $LiNbO_3$ this is best provided by the use of iron (Fe) impurities which are intentionally introduced during growth of the crystal[2,3].

Figure 1 shows an iron-doped crystal before and after the storage of a hologram. For storage to occur, some of the traps must be empty. The empty traps are Fe^{3+} ions which do not absorb light. The occupied traps are Fe^{2+} ions with a strong absorption band near 4880 Å, the wavelength used for recording. The concentration of the occupied and empty traps is determined by the doping level and by oxidation-reduction heat treatments[4]. In typical crystals, there are roughly 10^{18} cm^{-3} empty traps and 10^{17} cm^{-3} filled traps. The filled trap concentration is usually limited to this value or less so that the crystal does not absorb too much light, an effect that would prevent optimum readout of the holograms.

To record a hologram, the crystal is exposed to two interfering light beams of a wavelength (4880 Å) that is absorbed by the Fe^{2+} ions. The interference produces a sinusoidal light intensity pattern, shown in the bottom of Fig. 1. There is a corresponding pattern of free electrons generated by photoionization of the occupied traps. The free electrons migrate through diffusion or drift and a net space charge is built up. Figure 1 shows the situation for diffusion. Electrons excited into the conduction band diffuse toward regions of low light intensity. After several steps of excitation, diffusion, and retrapping, the trapped electrons are redistributed as shown. There is depletion in regions of high light intensity and accumulation in regions of low light intensity. This sets up a space charge field pattern that modulates the refractive index via the electro-optic effect of $LiNbO_3$. The result is a thick phase hologram.

The sensitivity of the storage process[4] depends on (a) the amount of charge separation generated by a given exposure to light and (b) the dielectric and electro-optic constants of the material. The latter properties are fixed for a given material and determine the index modulation that corresponds to a given space charge density[5]. The charge separation sensitivity can be varied, however, because it depends on the absorption state and charge transport properties of the crystal. These parameters are currently under investigation

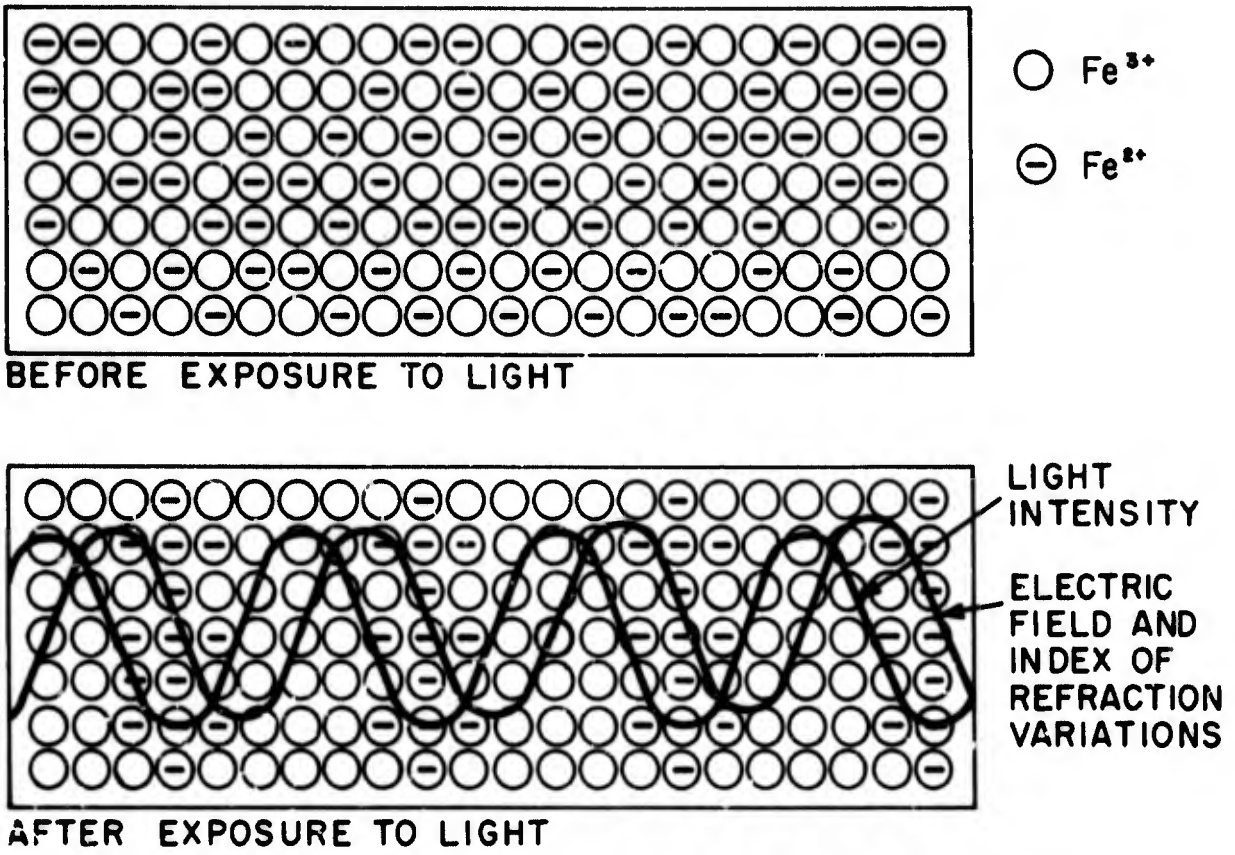

Figure 1. Mechanism for hologram storage in Fe-doped $LiNbO_3$. The electric field pattern creates a phase grating through the electro-optic effect.

in our materials research program which is aimed at improved storage performance in Fe-doped $LiNbO_3$[4]. At the present state-of-the-art, roughly 1 J/cm^2 of incident light (at 4880 Å) is required to record a hologram with ~40% diffraction efficiency in this material. It is interesting to note that this efficiency in a 1-cm-thick crystal of $LiNbO_3$ requires a space charge density of only 10^{15} cm^{-3}, well within the dynamic range of our crystals (nearly 10^{17} cm^{-3} trapped electrons are available for the storage process).

Holograms in these materials can be erased by exposure to a uniform light beam which excites all of the trapped charges and allows them to redistribute uniformly. This wipes out the space charge pattern and completely erases the hologram. The sensitivities for storage and erasure are not necessarily equal, and depend upon the hologram amplitude and the mechanism for storage (i.e., diffusion or drift). In typical crystals used in this program, erasure is much slower than storage, a behavior that is consistent with storage enhancement by what appears to be an optically generated electric field[4]. This situation is required for multiple storage, as will be discussed in Section III, but the optical erasure, although slower than storage, still allows the readout beam to eventually erase all of the holograms.

B. HOLOGRAM FIXING

One of the most important results of this program has been the development of an improved fixing technique suitable for recording optically stable holograms in Fe-doped $LiNbO_3$. Hologram fixing is a prime requirement for this program; the holograms must not erase or degrade during readout. Past studies of hologram fixing in electro-optic crystals centered on undoped $LiNbO_3$, but it has only been through recent advances in our program that the high sensitivity and dynamic range of Fe-doped $LiNbO_3$ can be utilized in the storage of fixed holograms.

Holograms in $LiNbO_3$ can be fixed by a simple heat treatment[6]. The process relies on the formation of an ionic charge pattern through drift of thermally activated ionic defects. The defects drift in the electric field pattern of the hologram so as to neutralize the electronic charge pattern generated by the light. At certain temperatures the ionic drift rate is larger than that of the electrons. The net result is an ionic pattern that perfectly mirrors the electronic pattern. Upon cooling to room temperature, the ionic pattern is frozen in and the electronic pattern of the original hologram is converted to an optically stable ionic pattern. The hologram is fixed.

Since the fixing neutralizes the space charge pattern the crystal must be illuminated before readout. The light tends to redistribute the electrons so that they no longer neutralize the ionic pattern. The electric field pattern then reappears and the hologram can be read out. The full diffraction efficiency cannot be recovered, however, because the electrons are prevented from complete redistribution by the ionic space charge field. Nevertheless, undoped crystals perform very well; nearly half of the original diffraction efficiency can reappear after fixing in these crystals[6,7].

Although undoped $LiNbO_3$ crystals are highly useful with the above technique, they are not sensitive and require a strong applied field ($\sim 10^4$ V/cm) to record multiple holograms. On the other hand, Fe-doped $LiNbO_3$, which normally has high sensitivity and good multiple storage performance, does not fix well with this technique. The diffraction efficiency after fixing is typically much smaller than that of the original hologram. Analysis carried out under our materials research program indicated that the problem was due entirely to the higher density of occupied traps in the doped crystals as compared with that of undoped crystals. During readout with a uniform light beam, the traps introduce sufficient photoconductivity to screen out a large fraction of the fixed ionic charge pattern. One can show[4] that, assuming sinusoidal patterns and a small modulation in the density of occupied traps, the net magnitude of the holographic space charge field is given by

$$E_{net} = E_o[1 + (e^2/kT)(n_t/\kappa^2\varepsilon)]^{-1} \qquad (1)$$

where E_o is the original (unfixed) field magnitude, e is the electronic charge, k is Boltzman's constant, T is the temperature, n_t is the density of trapped electrons (Fe^{2+} ions), ε is the dielectric constant, and κ indicates the

periodicity (sin κx) and is given by $2\pi/\ell$ where ℓ is the grating spacing. In our work ℓ = 1 μm which at room temperature gives

$$E_{net} = E_o \left(1 + n_t/1.6 \times 10^{15} cm^{-3}\right)^{-1} \quad (2)$$

In the doped crystals used here, n_t approaches 10^{17} cm^{-3}, and from Eq. (2) we see that the photoconductivity effect severely limits the net field available for readout.

To compensate, one must increase the magnitude of the initial hologram, i.e., increase the storage exposure, but this is prevented at room temperature by coupled wave[8] and optical damage[3] effects. These effects distort and degrade the reconstructed image to the point where it is no longer useful, even though it may have a reasonable diffraction efficiency after fixing.

The technique for overcoming this problem was developed under this program. All that is required is to record the holograms while the sample is at an elevated temperature (140°C to 190°C); i.e., storage and fixing are carried out simultaneously. The temperature and optical exposure are chosen such that the fixing rate equals or exceeds the storage rate. In this situation, ionic conductivity continually neutralizes the electronic space charge pattern as it is being recorded. As a result, large space charge fields cannot build up. Since these large fields are the origin of the index modulations that set up the beam coupling and optical damage problems, one can by the simple expediency of recording in hot crystals for a sufficiently long time, record fixed holographic patterns of sufficient magnitude to produce a usable diffraction efficiency for readout at room temperature.

The storage sensitivity for holograms fixed in this way is fairly good, but somewhat less than that for storage of unfixed holograms in the same crystals. Our results show that for $LiNbO_3$ doped with 0.01 to 0.05% of Fe, the exposure required for a fixed hologram is roughly 5 to 10 times that required to obtain the same efficiency for an unfixed hologram; i.e., 5 to 10 J/cm^2 is required to record a fixed hologram of ∿40% diffraction efficiency. We have not as yet observed any loss of dynamic range as compared with that of the unfixed holograms. Fixed holograms with close to 100% efficiency have been recorded with this write-while-hot technique, and this was done in crystals in which only ∿1% fixed holograms could be obtained by the previous technique. In fact, we have found that index modulations much larger than that required for 100% diffraction efficiency can be recorded with the write-while-hot technique. This is shown by the angular response of such a hologram in Fig. 2. The lack of a main peak and a preponderance of side lobes is consistent with a phase grating with an extremely high index modulation[9]. This is an important point for this project; a high dynamic range is necessary for full utilization of Fe-doped $LiNbO_3$ for multiple storage of fixed holograms.

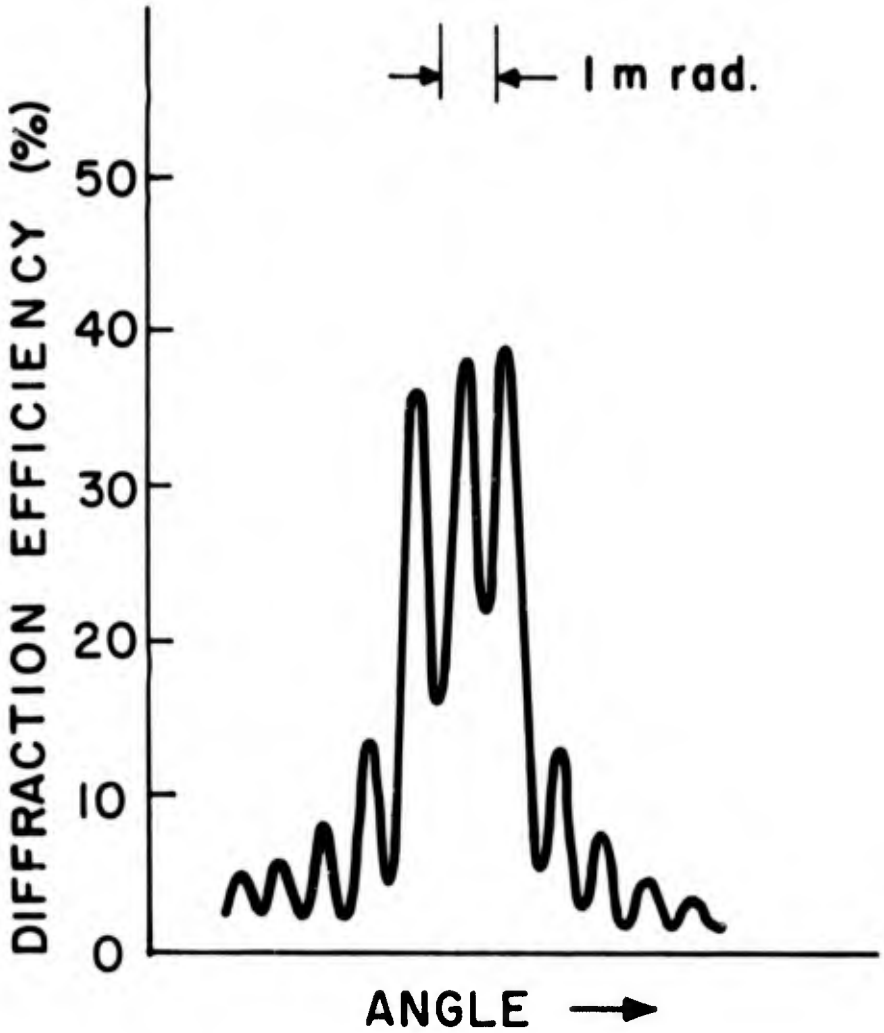

Figure 2. Diffraction efficiency as a function of readout angle for a fixed hologram in a 0.2-cm-thick crystal of 0.03% Fe-doped $LiNbO_3$. The large side lobes demonstrate the high dynamic range of this material for fixed holograms.

III. STORAGE TECHNIQUES AND LIMITATIONS

To achieve the goals of this program, the storage material must be capable of containing many holograms within its volume. Our initial approach in this area was to use undoped (or low doped) crystals of $LiNbO_3$ with which one can obtain a high capacity for multiple storage with the aid of an applied electric field, and then fix all holograms in "batch" with one heat treatment. We took another approach during the course of this program after the development of the "write-while-hot technique" described in the previous section. Our results described in this section show that this technique allows, in addition to high efficiency, a high capacity for multiple storage of fixed holograms in Fe-doped $LiNbO_3$.

A. STORAGE TECHNIQUE

There are two alternative techniques for multiple storage: the holograms can be recorded either simultaneously or sequentially. We use the latter method primarily for convenience. Simultaneous recording requires a complicated setup. In addition, the simultaneous technique may have severe problems concerning signal-to-noise ratio and hologram crosstalk because of the multiplicity of beams that are allowed to interfere during the storage process.

The sequential storage technique is best described with the aid of Fig. 3, which shows a $LiNbO_3$ crystal placed at the intersection of two 4880-Å beams from an argon laser. To record, one exposes the crystal to both beams, the reference beam and the object beam. The latter contains the information to be recorded, usually from a transparency placed in the beam. In order that the resulting hologram be fixed, the crystal must be maintained at an elevated temperature (> 120°C). We do this by attaching the crystal to a transparent resistive heater composed of a thin tin oxide layer on a piece of glass.

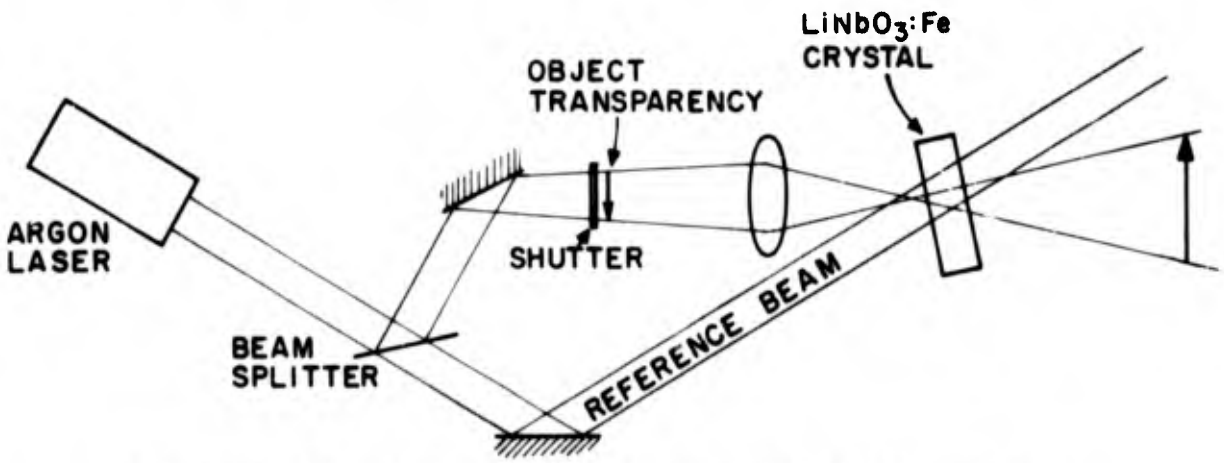

Figure 3. Recording apparatus for multiple storage. The sample is rotated (in the plane of the paper) to selectively store and access the different holograms.

When the holographic exposure is completed, the beams are turned off and the sample is rotated slightly in the plane of intersection. A new transparency is then placed in the object beam, and the new hologram is recorded. This procedure is repeated for each recording. The crystal is then cooled to room temperature and exposed to light to develop the electric field patterns as discussed in Section II-B. The holograms can then be accessed with the reference beam, one at a time, by rotating the sample.

The basic limitation of this technique is optical erasure during storage. Fixed holograms in $LiNbO_3$ are completely stable at room temperature, but can be optically erased at the fixing temperature. The light tends to redistribute the trapped electronic charge, and since the ions are also mobile at the elevated temperature, the net result is an optical erasure of both the ionic and electronic patterns. Erasure occurs during sequential recording of a number of fixed holograms in hot crystals of Fe-doped $LiNbO_3$, and such an experiment is a convenient way to measure the erasure. Figure 4 shows the room-temperature readout of two sets of holograms that were sequentially recorded at the indicated temperature. The first ones recorded (lower numbers) have been partially erased by the beams used to record subsequent ones (higher numbers). Thus, the gradual decrease of efficiency toward lower numbers is a measure of the erasure

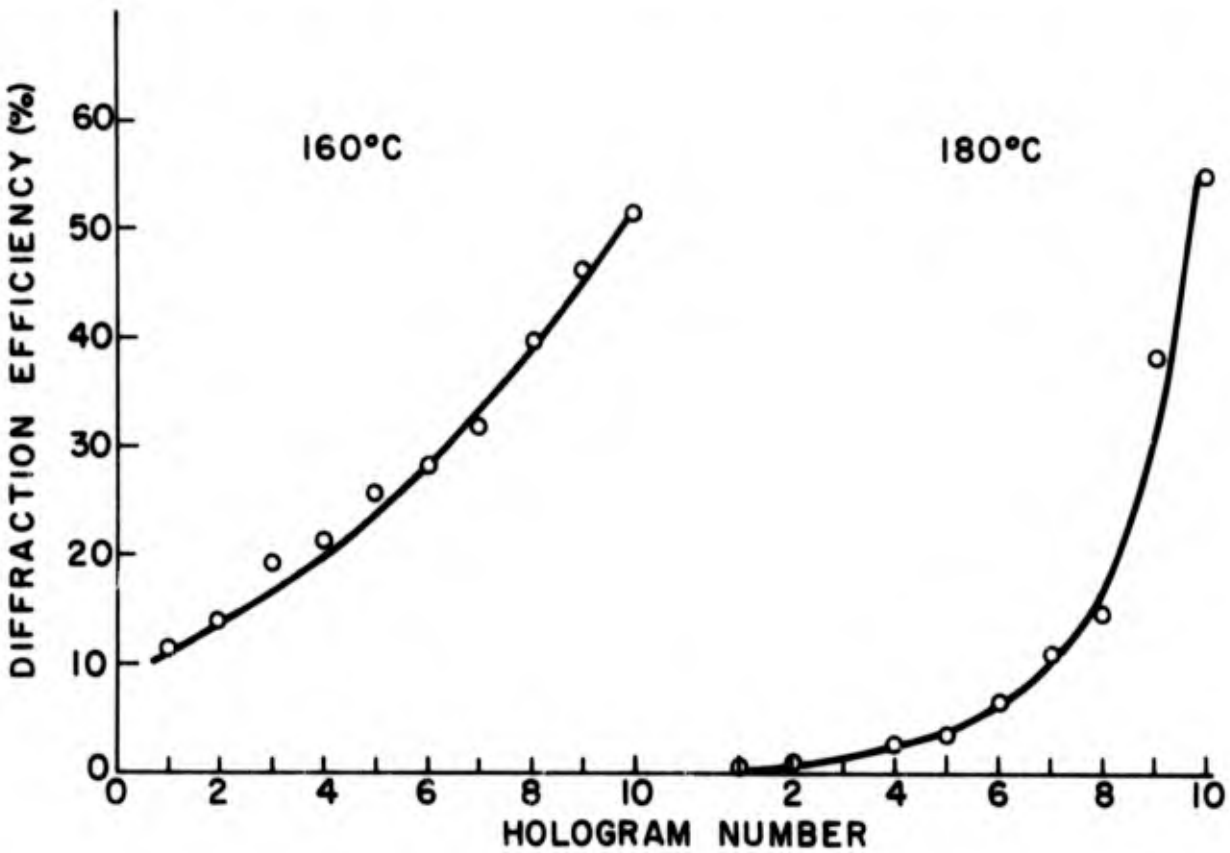

Figure 4. Diffraction efficiency of 10 fixed holograms, recorded at the indicated temperatures, and read out at room temperature for a 0.5-cm-thick sample of 0.01% Fe-doped $LiNbO_3$.

sensitivity. This effect is quite dependent on temperature; erasure at 180°C is much larger than that at 160°C. Thermal erasure may also contribute to this result. Note, however, that the storage sensitivity is the same for the two temperatures as evidenced by the efficiency of hologram 10. This is the last one recorded and should show no effect of erasure; it represents the storage sensitivity of the material.

B. STORAGE CAPACITY

In practice, the diffraction efficiency of the holograms must exceed a minimum value determined by the intensity of light required for detection, and the amount of light available for readout. For this reason, high-temperature erasure (optical or thermal) limits the number of useful fixed holograms that can be recorded in Fe-doped $LiNbO_3$.

The resulting limitation on storage capacity is calculated in Appendix A and is given by

$$\eta_n = \eta_1 \left[1 + (n - 1)/\beta_1\right]^{-2} \tag{3}$$

where n is the number of holograms, η_n is their diffraction efficiency, and β_1 is $\mathcal{E}_e/\mathcal{E}_1$, the ratio of the erase energy (the energy required to erase a hologram by ∿75%) to the write energy for a hologram with η_1 diffraction efficiency. This relationship was derived under the conditions that η_1 is the efficiency of the first hologram recorded in the sequence, and that all succeeding exposures are adjusted so that the erasure is compensated, i.e., all holograms have the same efficiency.

Using the above relationship, we can determine the storage capacity of Fe-doped $LiNbO_3$ from the erasure curves shown in Fig. 4. In this case, η_1 is ∿50% and β_1 is determined from the number of exposures required to erase a hologram by 75%. The latter number depends on the temperature used for storage, and is ∿15 for 160°C and ∿5 for 180°C. The appropriate curves of efficiency vs. hologram number are shown in Fig. 5 for different values of β. From these curves, we can see that for a β of 15, the situation for 160°C, one can record 100 holograms with more than 1% efficiency or 1000 with more than 0.01%. As discussed in Section VIII, this efficiency appears to be suitable for a vidicon pickup.

Since a lower temperature cannot be used without prohibitively slowing down the fixing process, the results show that for doping levels used here, 160°C is the optimum temperature for multiple storage.

It should be kept in mind that the above-mentioned calculation and experiments were for simple holograms, i.e., plane phase gratings. In actual practice, the effect of a transparency and object beam focussing must be taken into account.

It is interesting to note that the extremely high dynamic range of this material, although important for multiple storage, cannot in itself allow one

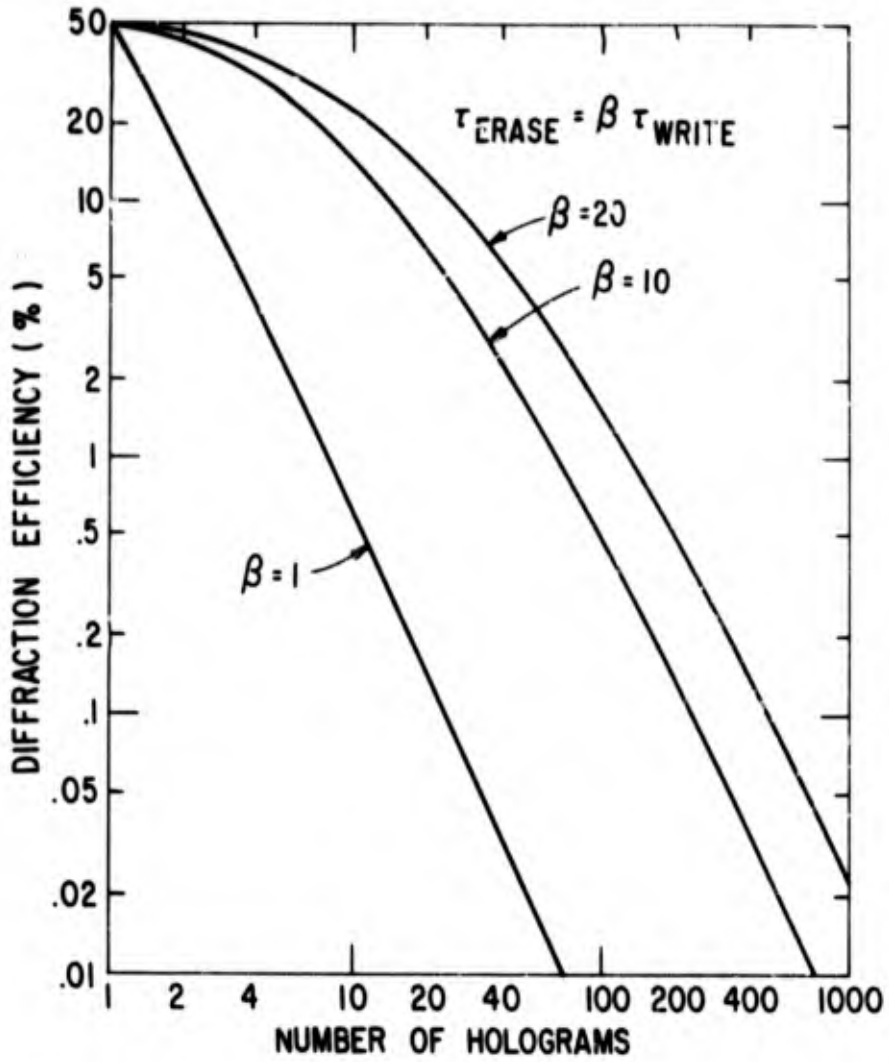

Figure 5. Multiple storage capability of Fe-doped $LiNbO_3$, with the write-while-hot technique. β depends on the temperature of recording and is a maximum at 160°C.

to significantly increase the efficiency of a given number of holograms. One could conceive of doing this by using for the first hologram an exposure that gives an index modulation much larger than that required for 50% efficiency. However, this is compensated by a corresponding decrease of β. Consider Eq. (3) in the limit where $n >> \beta$. In this regime we have

$$\eta_n = (\eta_1/n^2)(\mathcal{E}_e/\mathcal{E}_1)^2 \tag{4}$$

But since

$$\eta_1 = b\,\mathcal{E}_1^2 \tag{5}$$

where b is a constant that depends only on the storage sensitivity, we have for the efficiency

$$\eta_n = b\,\mathcal{E}_e^2/n^2 \tag{6}$$

a value that depends only on the storage sensitivity, the erasure energy, and the number of holograms. (We arbitrarily assume that the quadratic behavior for η_1 extends to efficiencies larger than 50%. This is, of course, not possible but it is a convenient way of deriving Eq. (6), which is valid for values of η_n less than 50%.) It must be kept in mind that Eq. (6) is also valid only in the regime where $\mathcal{E}_e$ is much larger than $\mathcal{E}_1$ (to allow the approximation used in Appendix A), but much smaller than $n\mathcal{E}_1$ [for the assumption of Eq. (5)].

IV. MULTIPLE STORAGE

A primary aim of this program is to store and fix 100 images in holographic form throughout a thick crystal of $LiNbO_3$. The attainment of this goal was greatly facilitated by the development under this program, and the associated materials research program, of the write-while-hot technique for use with heavily Fe-doped $LiNbO_3$. Using this method, we stored and fixed ten holograms with a diffraction efficiency of 15 to 20%, and 100 holograms, each with a diffraction efficiency greater than 1%. In this section, we discuss recording and fixing and the quality of the images obtained.

A. MATERIALS

The crystals used in this work were 0.01 to 0.03 mole % Fe-doped $LiNbO_3$ grown by W. Phillips of these Laboratories. The crystal growth and preparation techniques were discussed in an earlier report[4]. In particular, for the storage and fixing of ten holograms a 0.2-cm-thick crystal containing 0.015 mole % Fe was used while for the storage of 100 holograms 0.5-cm-thick crystals containing 0.01 and 0.03 mole % Fe were used.

The optical quality of these crystals was good to excellent except for the 0.01 mole % crystal which developed a discoloration during an oxidation process to decrease its absorption. This crystal was not used any further.

The absorption at 4880 Å arising from Fe^{2+} was kept at a level of $\sim$0.3 OD (50% transmission after correction for reflectivity losses) to strike a proper balance between sensitivity and the loss in the usable diffraction efficiency. Figure 6 shows an absorption spectrum for the 0.03 mole % Fe-doped crystal which was used for the storage of the 100 holograms.

B. EXPOSURE CRITERIA

The recording of a hologram at room temperature, or elevated temperature, partially erases those holograms recorded previously in the same volume. To record a large number of holograms with the same diffraction efficiency, the proper exposure times are those derived in Appendix A. These are given by

$$\mathcal{E}_n = \mathcal{E}_1 \beta_1/[(n-1) + \beta_1] \tag{7}$$

where $\mathcal{E}_n$ and $\mathcal{E}_1$ are the exposure levels of the nth and 1st hologram respectively, and β is the ratio of the erasure to storage exposures. The β was measured for the crystal used in the recording of the 100 holograms by recording and fixing 40 plane phase gratings. Figure 7 shows a trace of the diffraction efficiency obtained at room temperature for each hologram. Each one was recorded with a constant exposure at 160°C. The exponential character of the

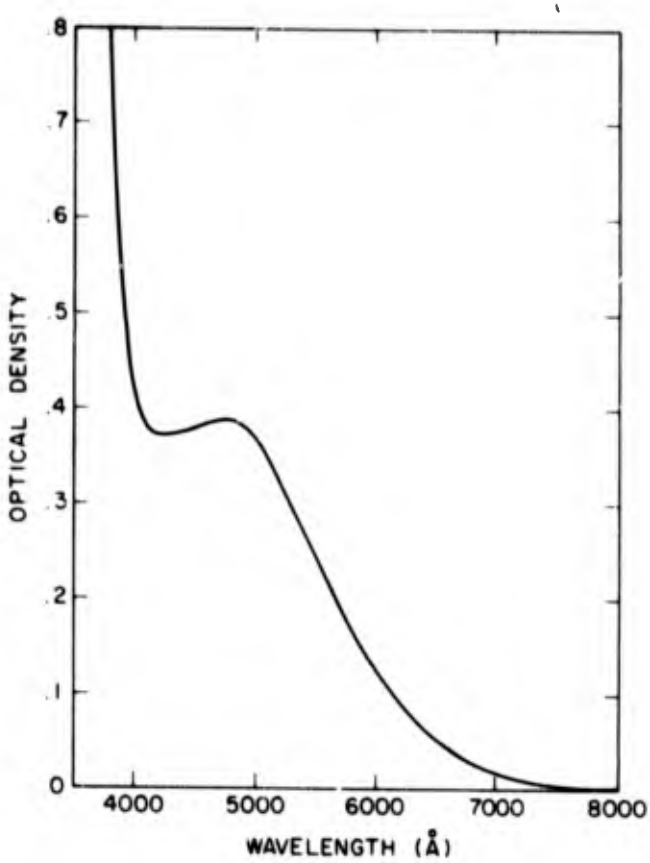

Figure 6. Optical absorption in a 0.5-cm-thick crystal of 0.03 mole % Fe-doped $LiNbO_3$.

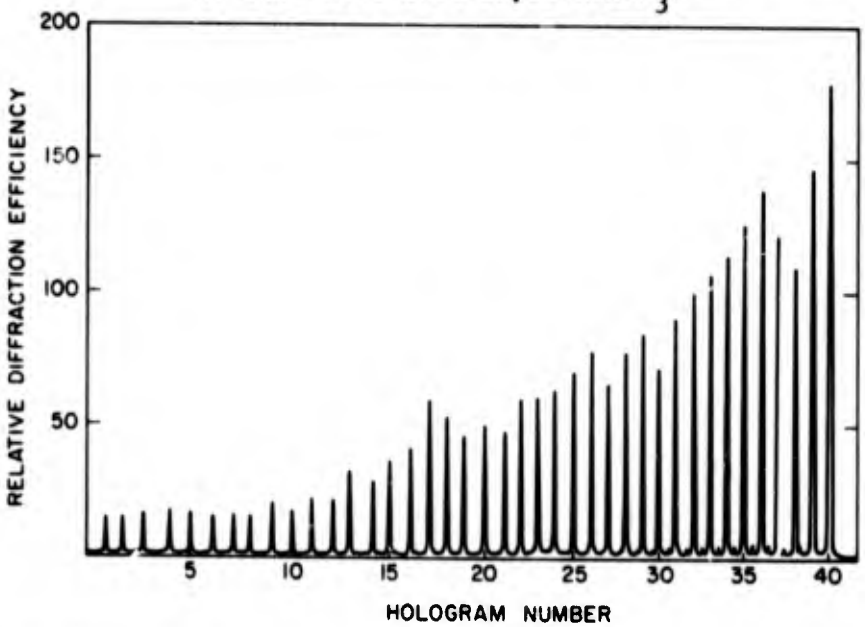

Figure 7. Relative diffraction efficiency of 40 holograms stored in the crystal shown in Fig. 6. The exposure for each hologram was the same.

erasure process is shown in Fig. 8 and verifies the assumption of Appendix A. From these results a write-erase asymmetry of $\beta = 15$ was calculated for the 0.03 mole % Fe-doped crystal. The asymmetry at elevated temperatures is then comparable to that obtained for these crystals at room temperature.

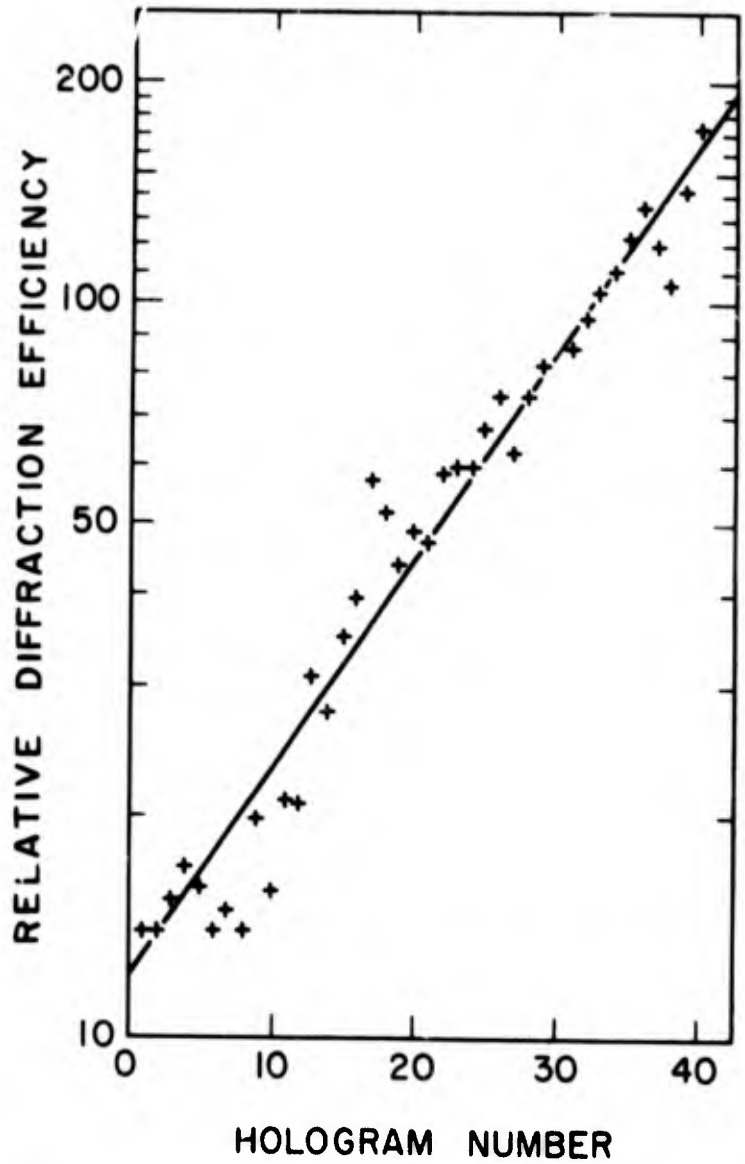

Figure 8. Exponential dependence of optical erasure during recording of subsequent holograms.

C. RECORDING SYSTEM

The recording arrangement used is shown in Fig. 3. This arrangement is similar to those used earlier except that the interferometer was considerably

enlarged to accommodate the film transport used to provide the object transparencies. The typical laser power used was 800 mW at 4880 Å. The power incident on the sample in the reference beam was 10.0 mW/cm^2 in a 1.5-cm-diameter beam. The power incident on the object transparency was 6.0 mW/cm^2.

The object transparencies used in this program were textual material, resolution charts, and aerial chart segments. The film was chosen for its minimum grain size at the optimum contrast ratio. The transparencies were recorded using a Bolex Model H16 Reflex 16-mm camera with a Nikkor Auto f/3.5 lens.

Fresnel holograms were recorded with a magnification of 16/1 to provide sufficient size to view the image directly. For vidicon pickup of the reconstructed image a magnification of ∿1.5/1 was used.

D. HOLOGRAM EFFICIENCY

The goal is to record 100 holograms with a diffraction efficiency of 1%. Care must be taken in the definition of the diffraction efficiency when used with high contrast objects such as textual material or line drawings. The practical specification of diffraction efficiency is in terms of the usable diffraction efficiency. This is the fraction of the incident readout beam which is diffracted into the image. This fraction will differ from the true diffraction efficiency of the holographic grating due to absorption of both the incident and diffracted beams and to reflection losses at the surfaces (∿30% in the case of $LiNbO_3$ in the absence of AR coatings). As discussed above, the absorption in the crystal is typically ∿50%. Combined with reflection losses this gives a ratio

$$\frac{\eta_{usable}}{\eta_{true}} \sim 1/3 \tag{8}$$

Another factor that influences the apparent or usable diffraction efficiency is the object transmission. High contrast objects such as those used in this work have a transmission of the order of 1% of the incident light. An extreme case would be a circular region of the object containing 1% of the area with a transmission of 100%. If we restrict ourselves to the transmitting area, then an image of uniform brightness would be reconstructed with an efficiency

$$\eta_{usable} \sim \eta_{true}\, e^{-\alpha d} \tag{9}$$

where α is the absorption constant and d is the crystal thickness. If the transmission of this area decreases the usable diffraction efficiency η also decreases as

$$\eta_{usable} = \eta_{true}\, T e^{-\alpha d} \tag{10}$$

where T is the fractional transmission of the object. The diffracted power P_d is then

$$P_d = \eta_{true} T e^{-\alpha d} P_R \tag{11}$$

where P_R is the incident power in the readout beam. Equation (10) is the definition of the usable diffraction efficiency that we will follow.

E. RESULTS

The program was significantly advanced by the record-while-hot technique developed and discussed in Section II. The first application of this technique was the simultaneous recording and fixing of ten images. Following this we have recorded up to 100 holograms in several different tests. We shall discuss here the results obtained for the ten holograms and those obtained for 100 holograms since they constitute the landmarks of this program.

Ten holograms were recorded and fixed in a 0.2-cm-thick crystal of 0.015 mole % Fe-doped $LiNbO_3$. The objects used were high contrast slides of aerial charts and textual material. The usable diffraction efficiency per hologram was 15 to 20%. The angular spacing between holograms was approximately one degree of rotation but varied significantly from this number. No effort was made in this test to optimize the packing of the holograms.

The image quality obtained was excellent as shown in the photographs of Figs. 9 and 10. These photographs were taken with the image projected onto a ground glass screen with a magnification of 20 from the storage volume. In Fig. 10 the textual material which appears in the background is crosstalk from a nearby hologram. This will be discussed below.

The crystal containing the ten holograms has been exposed essentially continuously to an argon laser beam or a tungsten filament lamp for a period of eight months with no degradation in either the image quality or the diffraction efficiency.

One hundred holograms of two plane wave beams, each with a usable diffraction efficiency of approximately 0.5%, were recorded in 0.5-cm-thick sample[10]. Since these holograms contained no information the image quality could not be evaluated. An estimate was made of the integrated contrast ratio by comparison of light intensity scattered into the acceptance angle of the detector when the Bragg condition was satisfied to the light intensity detected at a point between two holograms. The ratio of these intensities was in the range of 50/1 to 80/1. At the 80/1 level the background light intensity is comparable to that expected from scattering from bulk and surface imperfections[11]. This result indicates that the corresponding contrast ratio for a particular image may be quite high.

Figure 9. Photograph of image reconstructed from one of ten holograms recorded and fixed in Fe-doped $LiNbO_3$ using the write-while-hot technique.

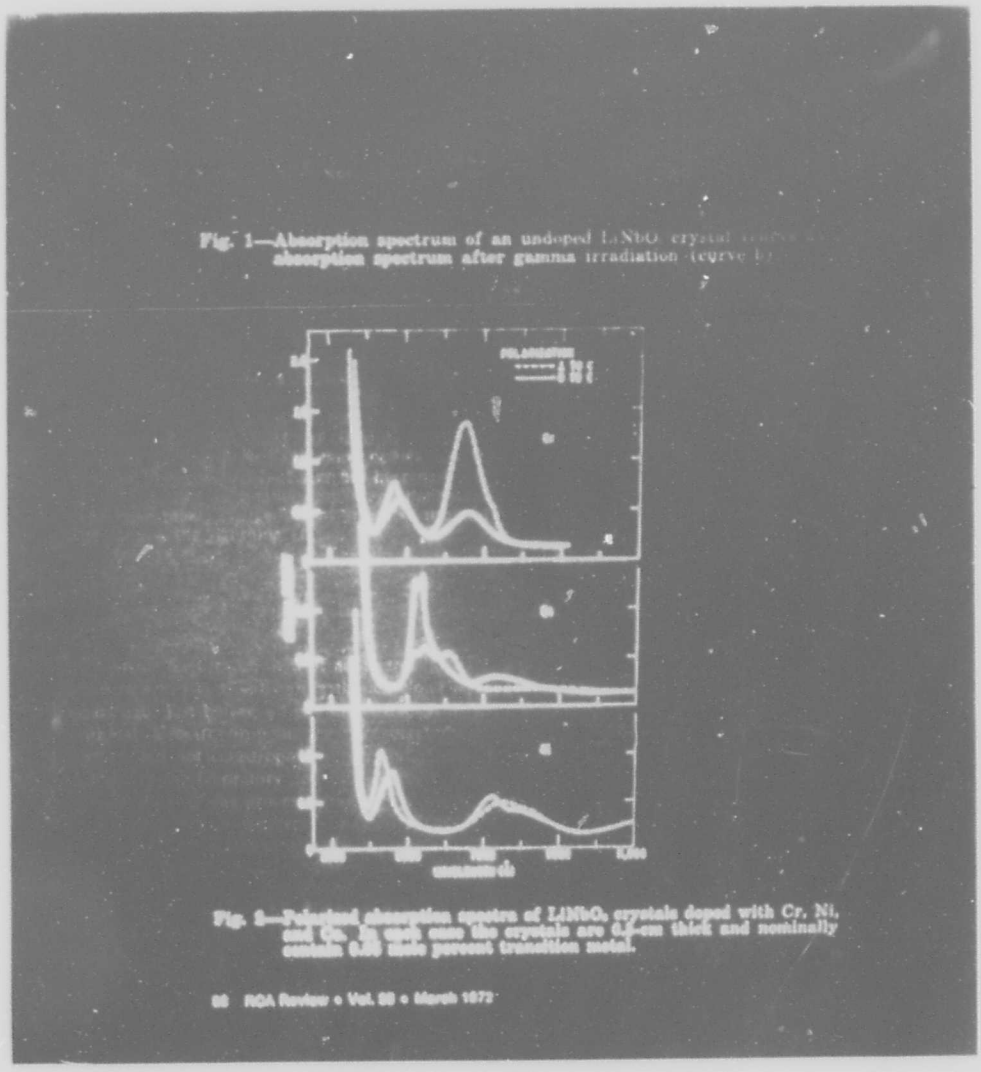

Fig. 1—Absorption spectrum of an undoped $LiNbO_3$ crystal [illegible] absorption spectrum after gamma irradiation (curve b).

Fig. 2—Polarized absorption spectra of $LiNbO_3$ crystals doped with Cr, Ni, and Cu. In each case the crystals are 0.5-cm thick and nominally contain 0.05 mole percent transition metal.

68 RCA Review • Vol. 33 • March 1972

Figure 10. Photograph of the image reconstructed from another hologram in the same crystal as shown in Fig. 9. Crosstalk from a neighboring hologram can be seen in the background.

One hundred holograms of monochrome images were recorded and fixed in a 0.5-cm-thick crystal. The galvanometer and associated electronics discussed in Section V of this report were used to provide angular addressing. For recording and fixing, the heater described in Section III of this report was used. For readout the crystal was mounted on a goniometer head for the galvanometer.

The fixed holograms each had a usable diffraction efficiency of 1%. The cosmetic quality of the images obtained was only fair to good. There are several reasons for this. Coherent noise such as bullseyes was present in the image due to diffraction and scattering from imperfections in the object transparency and the recording optics. The image intensity was also shaded due to nonuniformities in the recording beams.

The holograms were spaced in equal increments of approximately 3.5 mrad over a range of 20 degrees. This angular spacing corresponds to four times the zero to zero angular range of the main diffraction peak. The spacing was chosen to minimize linear crosstalk between holograms. Crosstalk was visible, however, in the reconstructed image due primarily to nearest neighbor holograms. Detailed studies of the effect of crosstalk on the image quality were not made during this program.

Measurements on the crystal in which the 100 monochrome images were recorded showed that a weak image of a hologram could be detected up to two angular spacings away from the correct angular address. The ratio of the diffracted power at the Bragg angle to that at the nearest neighbor angular addresses was measured to be in excess of 50/1 which is consistent with the measurement for the plane wave hologram discussed above. This result, while it does not give a measure of image quality, does indicate that usable contrast ratios can be obtained at this storage density.

F. STORAGE CAPACITY

The results discussed above are consistent with the theoretical predictions for a write-erase asymmetry $\beta \gtrsim 15$. The extension of these results to the level of 1000 holograms predicts a usable diffraction efficiency of $\sim$0.01%. Based on recent studies of the write-erase asymmetry, it does not appear likely that significantly higher values of β will be obtained.

At a storage density of the order of 1000 holograms, the foreseeable problems divide themselves into two classes. The first concerns the straightforward problems of detector sensitivity, extraneous light scattering from the storage medium, the retrieval system required, and the angular range over which the holograms are stored. In the second class are the more subtle problems of the required image quality as defined by the signal-to-noise or contrast ratio. The major contributions to image degradation, in addition to coherent scattering of light in the recording and readout optics and the storage medium, are linear crosstalk between holograms and fluctuations in the diffracted light intensity arising from a statistical distribution of the trapped charges which produces the holographic grating[12]. A tradeoff will most likely occur between these two noise components. The magnitude of the crosstalk will decrease with decreasing diffraction efficiency since the relative contribution

of the side lobes to the integrated diffracted light from a given hologram also decreases[9]. The results shown in Fig. 2 are an extreme example at high diffraction efficiencies. The contribution from statistical sources should, however, increase with decreasing diffraction efficiency since the number of trapped charges involved in the formation of a particular grating is smaller. Experimental studies have not been made of the relative importance of these effects since, until the present program, a suitable storage medium has not existed.

In conclusion, it appears that storage of 100 holograms is feasible in heavily Fe-doped $LiNbO_3$. The angular packing density can be reduced significantly from the level used in this program to reduce crosstalk between holograms. The upper limit to the storage capacity in the range up to 1000 holograms will be determined by the signal-to-noise ratio required for a given application.

V. RETRIEVAL TECHNIQUES AND DEVICES

One of the primary advantages of a volume holographic storage system is the simplicity of retrieval of stored images. To address a given hologram it is necessary to vary the angle of incidence of the readout beam on the storage medium. Acousto-optic or electro-optic light deflectors or mechanical devices such as galvanometers or stepping motors can be used for this purpose. In a previous program[11] the use of an acousto-optic deflector to provide random access of up to ten holograms was demonstrated, and the capabilities of these deflectors for use in larger systems were evaluated. In the present program mechanical devices were evaluated as components for retrieval. Only galvanometers were found to possess the high-speed, random-access capability required for a read-only memory at the level of 100 holograms.

This section contains a discussion of (A) the sensitivity and control required in a retrieval system, (B) the galvanometer system constructed, (C) the results obtained, and (D) some conclusions reached on the basis of these results.

A. ANGULAR SENSITIVITY

The degree of control required for random-access retrieval system depends upon the thickness of the storage medium, the repeatability of the accessing device, and the allowable fluctuation of the diffraction efficiency from image to image due to inaccurate angular positioning. The angular sensitivity of the diffraction efficiency η is determined from the relationship[9]

$$\eta = \frac{\sin^2(\zeta^2 + \nu^2)^{1/2}}{(1 + \zeta^2/\nu^2)} \tag{12}$$

The quantity $\zeta = 2\pi n_o d\delta \sin\theta_o/\lambda$ is a measure of the phase shift induced by moving off the Bragg angle, $\delta = \theta - \theta_o$ is the change in angle, n_o is the index of refraction, d is the hologram thickness, θ_o is the Bragg angle, and λ is the wavelength. $\nu = \pi\Delta n d/\lambda\cos\theta_o$ is the phase shift arising from the electronic or ionic space charge pattern and is a constant for a recorded hologram. Δn is the maximum index change in the recorded pattern. When the Bragg condition is satisfied, $\delta = 0$ and we obtain

$$\eta = \sin^2\nu = \sin^2(\pi\Delta n d/\lambda\cos\theta_o) \tag{13}$$

The behavior of the rolloff in diffraction efficiency with angle is given by Eq. (11) and is shown in Fig. 11 for a 0.65-cm-thick crystal. The angular

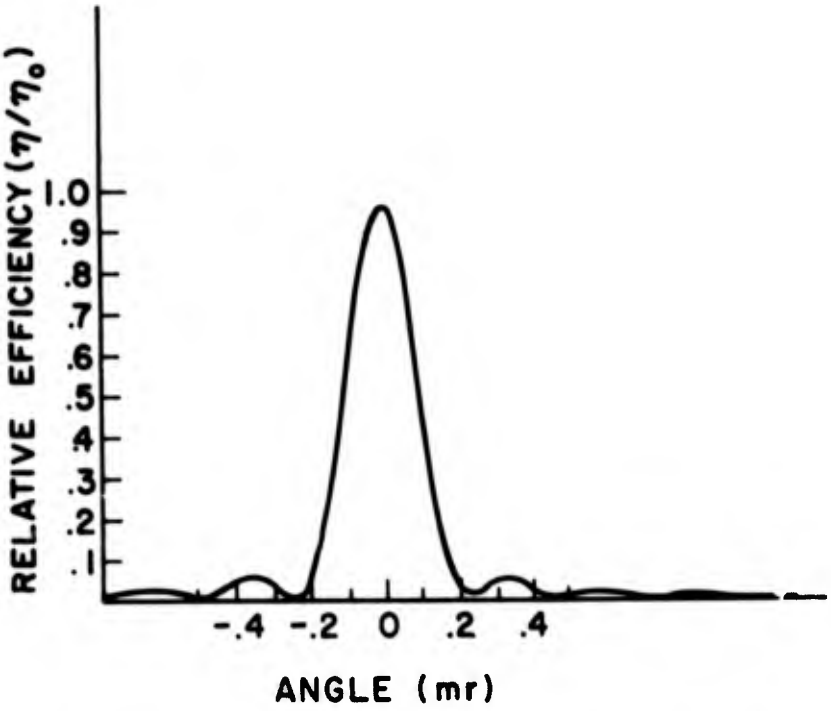

Figure 11. Variation in diffraction efficiency with angle for a hologram stored in a 0.65-cm-thick crystal of $LiNbO_3$.

deviation at which the first zeros in the diffraction efficiency occur can be approximated by

$$\Delta\theta = \frac{n\lambda}{2d} \frac{\cos\theta_o'}{\cos\theta_o \sin\theta_o} \tag{14}$$

A calculation of the rolloff using this equation is shown in Fig. 12. For a 1-cm-thick crystal of $LiNbO_3$, the first zeros for a hologram recorded at 0.488 μm with a Bragg angle $\theta_o = 15°$ occur at $\pm$ 0.22 mrad. For a 0.5-cm-thick crystal the first zeros are at $\pm$ 0.44 mrad. To obtain a readout efficiency greater than 50% of the peak diffraction efficiency ($\Delta\theta = 0$), the repeatability of the accessing device must be $\pm$ 0.22 mrad or less for the 0.5-cm-thick crystal.

B. COMPARISON OF DEVICES

In this program, mechanically accessed devices were investigated as opposed to electronically accessed (acousto-optic[11] or electro-optic) devices. Two types of devices were examined: galvanometers and stepping motors. The criteria used in evaluating their relative merits were: linearity, repeatability, speed of response, and a capability for use in a closed servo loop.

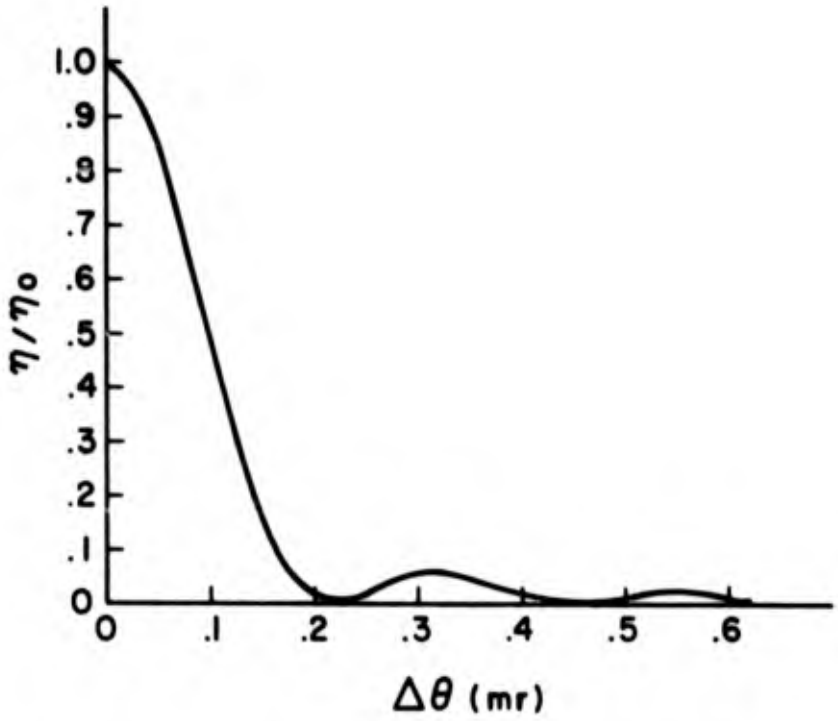

Figure 12. Theoretical variation in diffraction efficiency as calculated from Eq. (14) for a 1-cm-thick crystal of $LiNbO_3$.

1. Stepping Motors

Stepping motors possess the required repeatability and linearity in those cases where high accuracy is not required (crystal thickness less than 0.3 to 0.4 cm). For use in a servo loop the available stepping motors would require extensive gearing down to have a large number of steps between holograms. This requirement significantly increases the accessing time but does permit digital feedback control.

2. Galvanometers

The galvanometer currently used for light deflection applications is an analog device that possesses several of the characteristics required for a retrieval system. Random access of different angular addresses is possible as opposed to the sequential stepping process required with the stepping motor. The repeatability of using commercially available galvanometers is sufficient with holograms about 0.5 cm thick.

The major difficulty of employing a galvanometer in a retrieval system is hysteresis. To maintain the repeatability required, the galvanometer must be driven in the same direction to a given angular position. This, while not a serious problem in scanning applications, presents a complication for a random-access system. In particular, it slows the response time to

periods as long as 10 msec, because the galvanometer must be cycled through its complete loop during each accessing cycle to ensure the same starting position in each cycle. The method chosen here to accomplish this is discussed below; a detailed study of the minimum cycle time has not been made as yet.

While the galvanometer possesses several of the basic attributes required for use in a random-access retrieval system, several objections can be raised to its use under severe environmental conditions. The first of these is its poor mechanical stability. Next is the temperature dependence of the sensitivity; e.g., temperature changes greater than 5°C will produce shifts sufficiently large to require feedback control on the angular position for crystals thicker than 0.3 to 0.4 cm. Despite its drawbacks, however, comparison of the relative merits of the stepping motors and galvanometers led to the choice of the galvanometer as the best device for mechanical access. This choice was based on the relatively fast random-access capability and potential compatability with simple feedback loops.

C. ELECTRICAL CIRCUIT

The basic function of the electrical circuit for random access of up to 100 angular addresses is to control the voltage programable power supply that, in turn, drives the galvanometer (General Scanning, Model G330), as shown in the block diagram of Fig. 13.

Figure 13. Block diagram of retrieval system.

The stability and reproducibility of the angular position of the galvanometer depend directly upon the voltage generated by the addressing electronics. The requirements on the programing voltage can be estimated in the following way. The angular deflection of the galvanometer is given by

$$\theta = KI = K\ V/R \tag{15}$$

where K = 0.5 rad/mA is a constant for the galvanometer, I = V/R is the current through the galvanometer, R = 8 ohms is the coil resistance, and V is the voltage applied to the galvanometer. For a power supply with a programing constant of 1 V/V the addressing voltage is

$$V = R\theta/K = (16\ \text{V/rad})\ \theta \tag{16}$$

The required stability of the voltage is

$$\Delta V = (16\ V/\text{rad})\Delta\theta \tag{17}$$

For $\Delta\theta$ = 0.1 mrad ($\sim$1/9 of the zero-to-zero distance on the main peak of a 5-mm-thick hologram)

$$\Delta V = 1.6\ \text{mV} \tag{18}$$

The addressing electronics discussed below have measured drifts, due to all causes, of $\sim$0.2 mV over a period of days after a warmup of several hours. This corresponds to $\sim$1/70 of the zero-to-zero angular width of the hologram used here.

The current supplied to the galvanometer must drive it from -15° to + 15° about its rest position. Since the power supplies used are monopolar and since a positive programing voltage must be applied to the main power supply, switching is required. This is accomplished by generating a programing voltage of the form shown in Fig. 14 and reversing the direction of current flow through the galvanometer when the addressing voltage reaches zero.

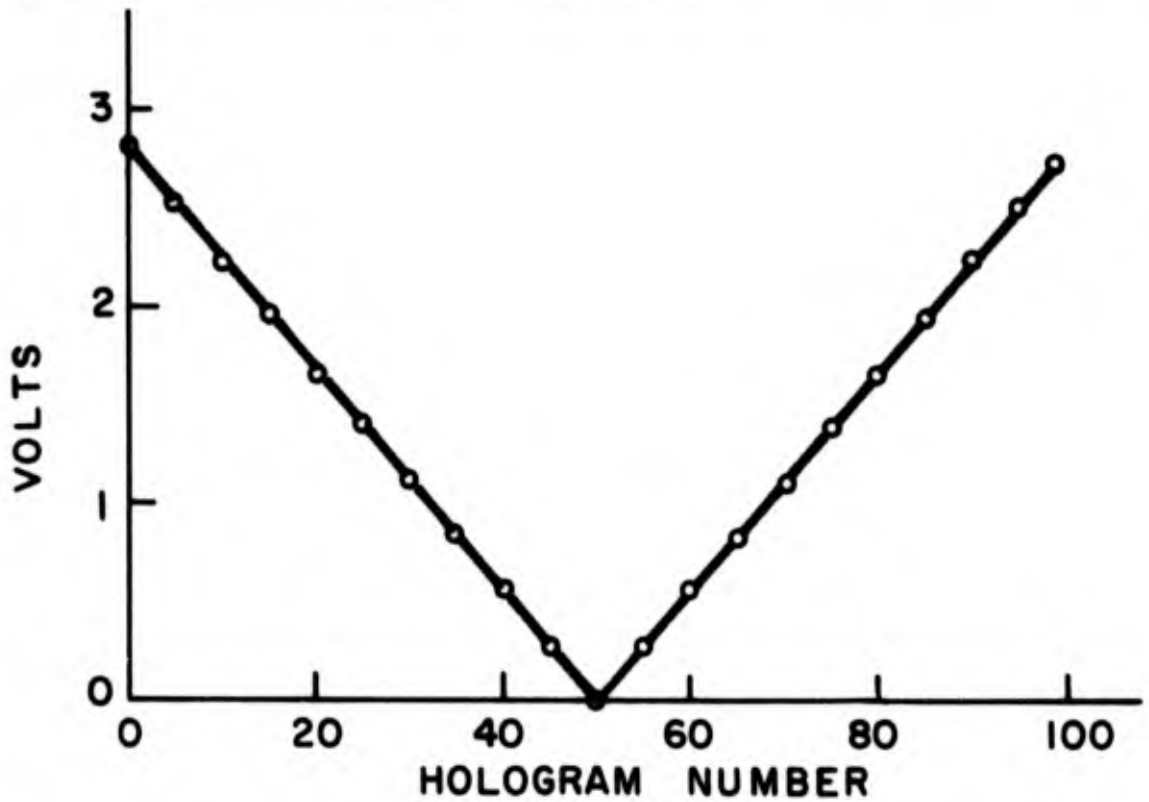

Figure 14. Voltage waveform used to program the power supply which drove the galvanometer.

The retrieval system was designed for a total of 100 angular addresses. The circuit diagram for the generation of the programing voltage is shown in Fig. 15, the circuit for the switching gear in Fig. 16. The voltages are generated from parallel resistance ladders, one corresponding to the ten's digit and the second corresponding to the unit's digit. These voltages are summed in the buffer amplifier A2 (Philbrick-Nexus 1003) and fed to the voltage programable supply (Lambda Model LR612A-FM). The voltage corresponding to the ten's digit is summed with a gain of 1, and the voltage corresponding to the unit's digit with a gain of 0.1.

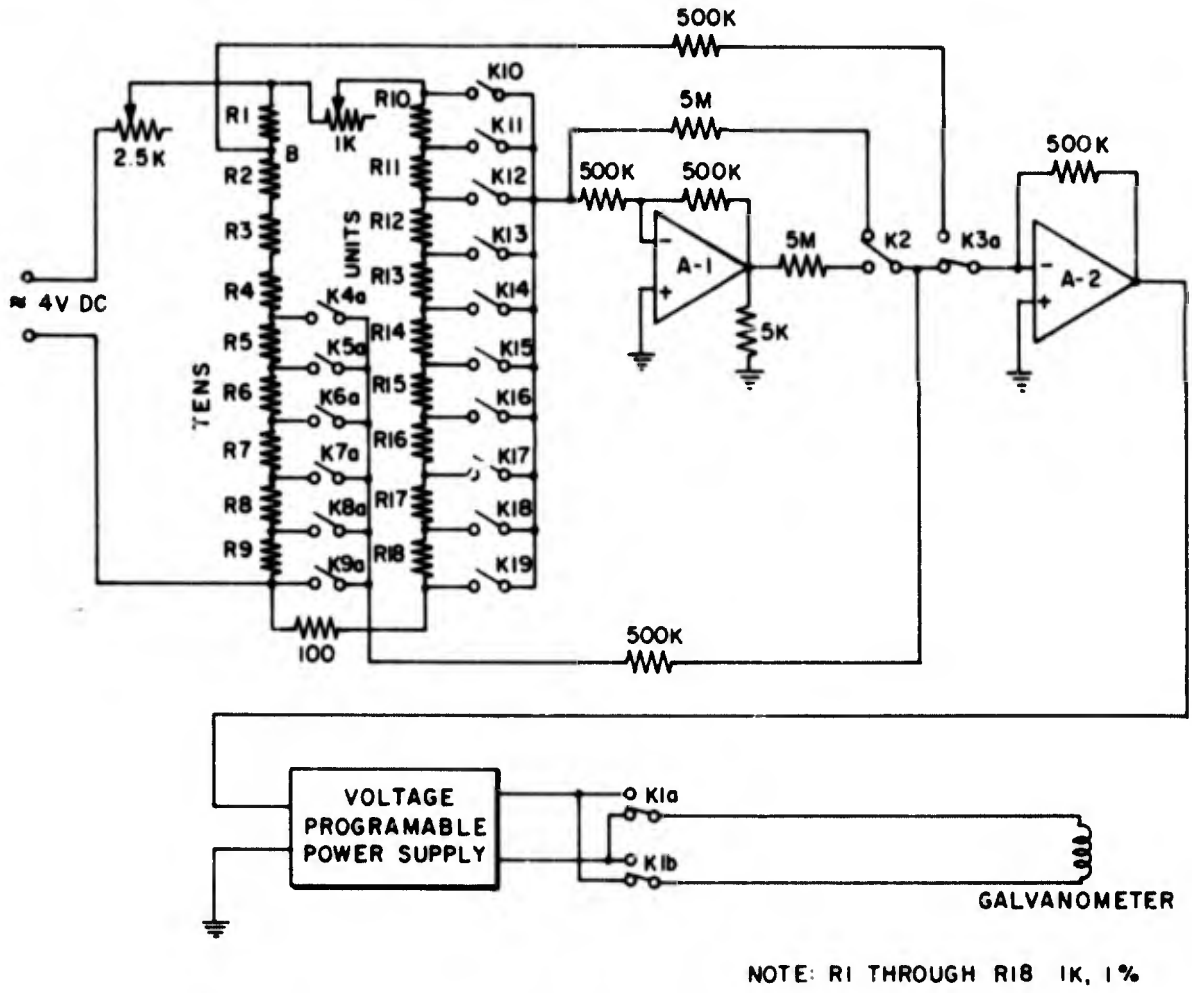

Figure 15. Circuit diagram of programing supply used to select one of 100 angular addresses.

To generate the voltage form shown in Fig. 14 several additional steps must be taken. For hologram numbers less than 50, relays K4 through K9 generate voltages corresponding to the ten's digits 0 through 5, respectively. For hologram numbers 50 and greater the relays K8 through K4 generate voltages corresponding to the ten's digits 6 through 9, respectively. For hologram

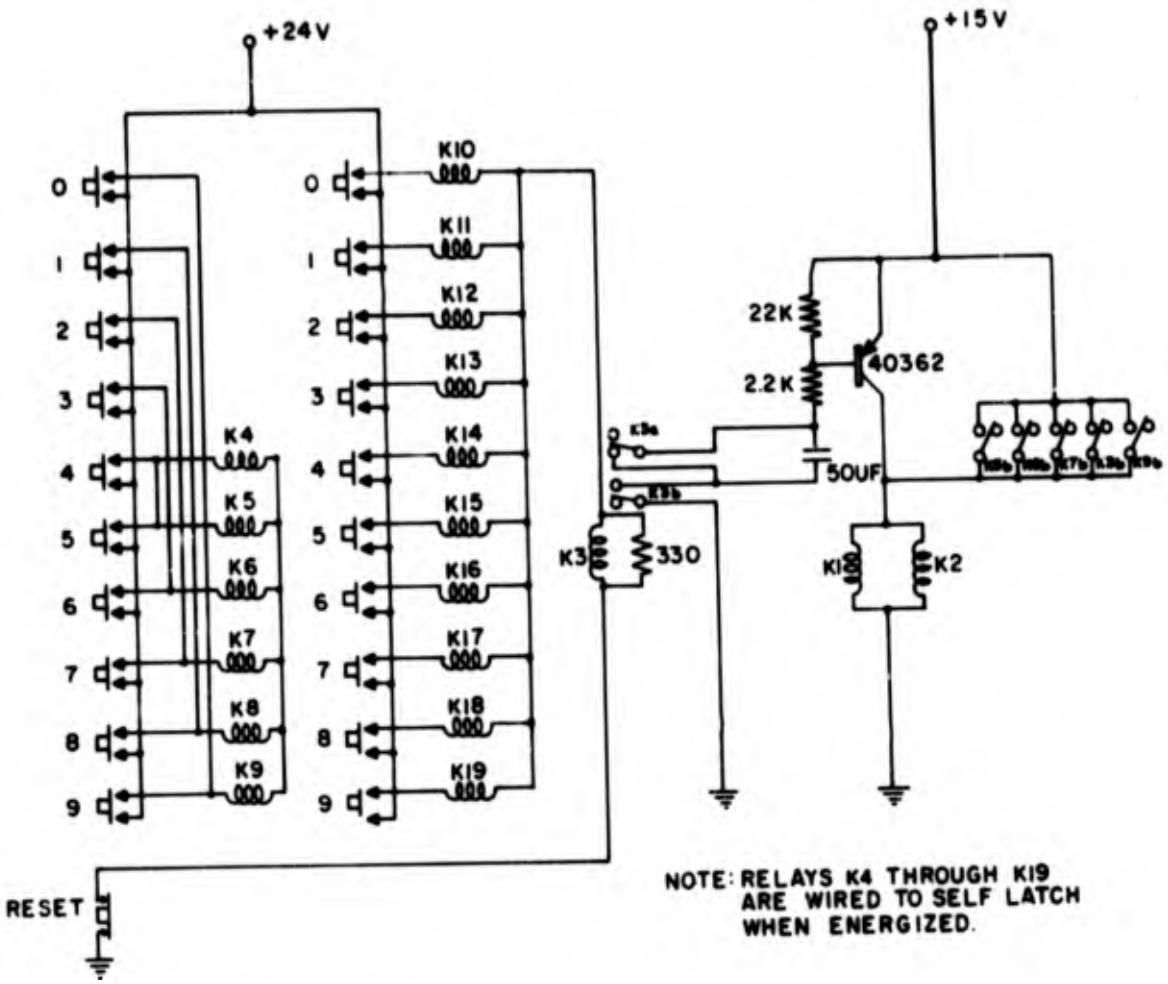

Figure 16. Switch circuit for programing voltage supply.

numbers less than 50 the voltage corresponding to the unit's digit must be subtracted from that of the ten's digit because of hysteresis effects. This is done by latching switch K2 to the output of amplifier A1 (Philbrick-Nexus 1003) which inverts the polarity before summing it in A2. For hologram numbers greater than 50 switch K2 is latched directly to the ladder through the 5-MΩ input resistor.

For the voltage ramp shown in Fig. 14 to drive the galvanometer from - 15° to + 15° the direction of current through the galvanometer must be reversed. This is done by latching relay K1 in one direction when the ten's digits 0 through 4 are selected and in the other direction when the ten's digits 5 through 9 are selected.

To switch from one hologram to another the galvanometer must first be cycled through its complete loop to maximum positive deflection and then to maximum negative deflection. To accomplish this, a clear switch is activated to release relays K4 through K19 and to latch relay K3 to position B on the

ten's ladder and relay K1 for positive deflection for 100 msec; the switch is then released to the position for maximum negative deflection.

The operational linearity of the accessing electronics is shown in Fig. 14. The linearity of the angular motion is shown in Fig. 17 where the deflection

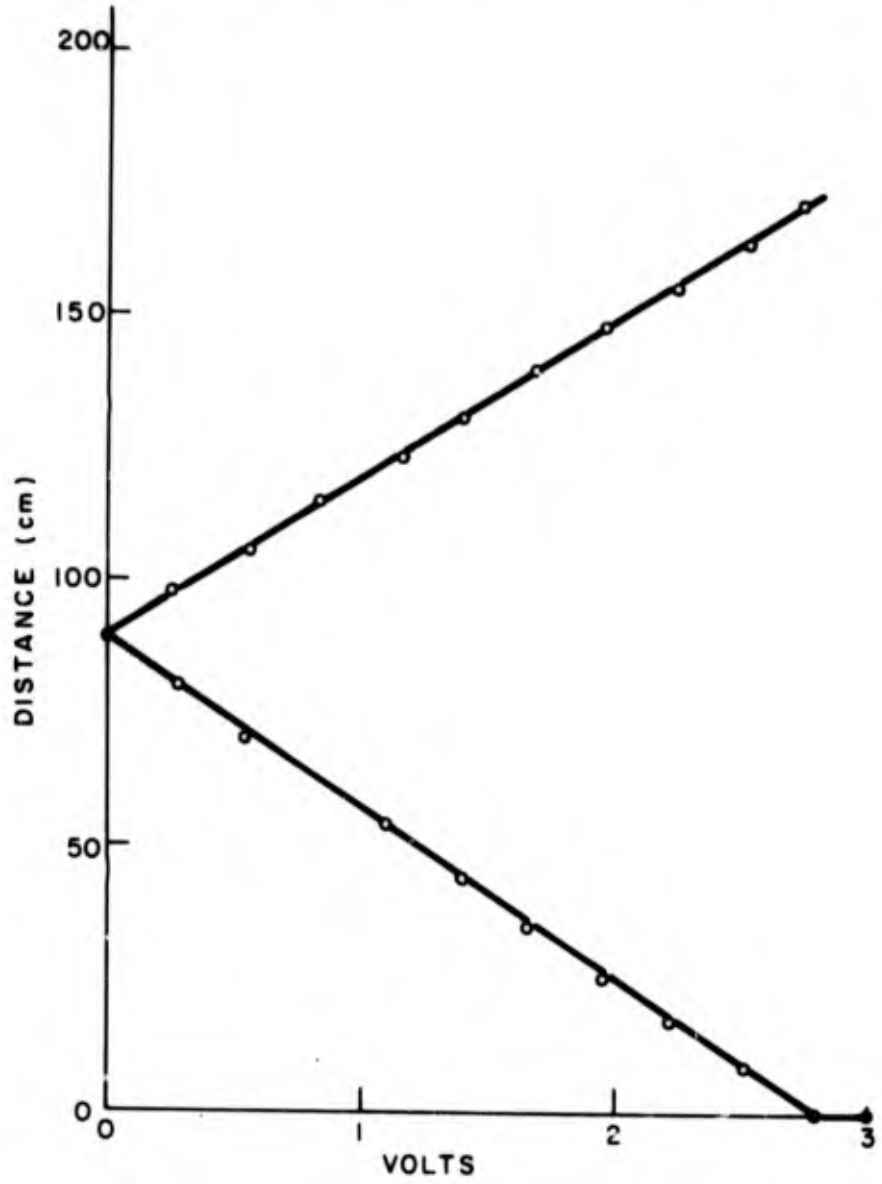

Figure 17. Linearity in angular deflection as a function of programing voltage measured on an arc with a 3.5-m radius of curvature.

was measured on an arc at a distance of 3.5 m from the galvanometer. A more sensitive test of the linearity was the following: Six holograms were recorded at six widely spaced angular addresses. The galvanometer assembly was then

rotated to produce the readout of one of those holograms up to ten addressing steps away from its original address. All other holograms were found using addresses ten steps away from their original addresses. There was no significant change in the diffraction efficiencies of the holograms with the change in angular address but the repeatability of retrieval of a given hologram was poor.

D. READOUT OF FIXED HOLOGRAMS

Holograms were recorded and fixed in $LiNbO_3$ using the write-while-hot technique. The retrieval system discussed above was used to rotate the crystal to different angular addresses with equal steps between holograms. However, since the holograms are recorded at one temperature and read out at another temperature, thermal expansion of the holographic grating will produce a change in the required angle of incidence between recording and readout.

To examine this problem one starts with the Bragg condition:

$$\lambda' = 2\, d_o \sin \theta \tag{19}$$

where λ' is the wavelength, d_o is the grating spacing, and θ is the angle of the readout beam away from the grating direction. The primed symbols indicate values in the storage medium. The form of this equation is identical in air; thus, the grating spacing d_o is independent of the ambient. If d_o is the grating spacing at room temperature, the Bragg equation at high temperature becomes

$$\lambda' = d_o\, (1 + \delta) \sin (\theta + \Delta\theta) \tag{20}$$

where $\delta = \alpha\Delta T$ is the fractional expansion in d_o, α is the coefficient of thermal expansion (from ref. 13: $\alpha_c = 2 \times 10^{-6}$, $\alpha_a = 16 \times 10^{-6}$), and ΔT is the difference in temperature between the recording temperature and the room temperature ($\Delta T \approx 140°C$). Expanding $\sin (\theta + \Delta\theta)$ and rearranging the terms in Eq. (20) gives

$$\frac{\lambda'}{d_o} - \sin \theta = \delta \sin \theta + (1 + \delta)\, \Delta\theta \cos \theta$$

Then

$$\Delta\theta = -\left(\frac{\delta}{1 + \delta}\right) \tan \theta \tag{21}$$

for the change in Bragg angle when recording at high temperature. The negative sign indicates that the Bragg angle is smaller at high temperatures. The assumption underlying this result is that the tilt angle of the grating to the crystal surface does not change with temperature.

Thus, after recording at T = 160°C and cooling to room temperature the Bragg angle must be increased to read out the hologram. For $\theta = 15°$ this implies a shift (using $\alpha_c = 2 \times 10^{-6}$) of $\Delta\theta = 0.086$ mrad. This shift is a constant of the recording geometry in that once θ (the half-angle between the recording beams) is fixed, $\Delta\theta$ is determined. To compensate for this increase in readout angle the crystal can simply be rotated by $\Delta\theta$.

E. RESULTS

In the recording process equally spaced angular addresses are required for compatibility with the retrieval system. The simplest solution was, then, to use the same galvanometer for recording as for readout. The only variant from galvanometer to galvanometer is the sensitivity constant given $k = \theta/I$, where θ is the angle and I the current. Therefore, holograms could be recorded in a crystal using one galvanometer and read out with another by simply changing the range of currents involved.

In a 0.5-cm-thick crystal, the results showed that one could reproduce an angular address within approximately the full width of the main diffraction peak, which corresponds to a galvanometer repeatability of approximately 0.25%. This is to be distinguished from the case where, in a group of holograms, several had angular addresses that were inconsistent with the remainder. This effect presumably arises from changes in the galvanometer sensitivity due to mechanical or thermal causes during the recording process. These changes cannot be detected when they occur since the hologram itself cannot be observed during the recording process when the write-while-hot technique is used.

For this reason random retrieval of 100 holograms was found to be impossible using the system discussed in this report. This conclusion indicates that other, more stable, accessing systems could be satisfactory. It is also possible that other causes, not as yet recognized, may also be contributing to this problem.

F. CONCLUSIONS

The results obtained during this program indicate that for storage media up to 0.5 cm thick a galvanometer can be used with reasonable but not satisfactory results. Due to the high angular selectivity for hologram readout and the random-access requirement, the necessary stability of power supplies and the sensitivity of the galvanometer to mechanical and thermal effects, the use of galvanometers is of questionable utility in a holographic memory.

VI. INCOHERENT READOUT

The use of an incoherent source such as a xenon or mercury arc or a tungsten filament for the retrieval of holograms stored in an electro-optic medium would have obvious advantages for a moving map display. In a previous investigation[11] we found that holograms stored in an electro-optic medium could be retrieved with an incoherent source, and the spectral content of the image and angular dependence of the efficiency were measured. The results of that investigation were sufficiently encouraging to warrant further investigation of this retrieval technique. In the following we will discuss additional measurements that we have made, and the conclusions that we have reached about the viability of incoherent readout in a hologram retrieval system based on an electro-optic storage medium.

A. HOLOGRAM FORMAT

Focused-image holograms were chosen for this work since they minimize the spatial coherence requirements on the readout source. In a thick recording medium the image is actually only in focus at one plane unless the depth of field is particularly large. Strictly speaking, therefore, the stored hologram is thus a quasi-focused image hologram. The holograms studied were recorded and fixed in crystals of Fe-doped $LiNbO_3$ approximately 0.2 cm thick. The ability to fix holograms in this material considerably simplified the task of measurement of the parameters of the readout process.

B. MEASUREMENT APPARATUS AND PROCEDURE

The recording and readout arrangements used for the study are essentially the same as those discussed in a previous report[11]. The readout system shown in Fig. 18 differs only in the use of a 1000-W xenon arc as a source and of interference filters to provide a narrow ($\sim$60 Å full width at half maximum) band of wavelengths.

The brightness of the readout beam and the reconstructed image was measured using a Pritchard photometer (Spectra Model 1970-PR). For both the readout beam and the image, the brightness measured was that of the light reflected from a $MgCO_3$ block which behaves as a Lambertian reflector. With this technique both the readout efficiency and the photometric brightness of the image can be measured with a minimum amount of correction required.

In the results discussed below a collimated reference beam was used since it was felt that this was the simplest configuration to reproduce. The results will not be affected by the choice of recording and readout beams with other focal properties as long as they are identical. It was found, however, that if a collimated reference beam was used for recording, a collimated reference beam gave the optimum readout efficiency. If, for a hologram recorded with a collimated reference beam, the readout beam was focused to increase the intensity of the light incident on the crystal, then the readout efficiency decreased. In the tradeoff between increasing incident light and decreasing efficiency the intensity of the diffracted light decreased.

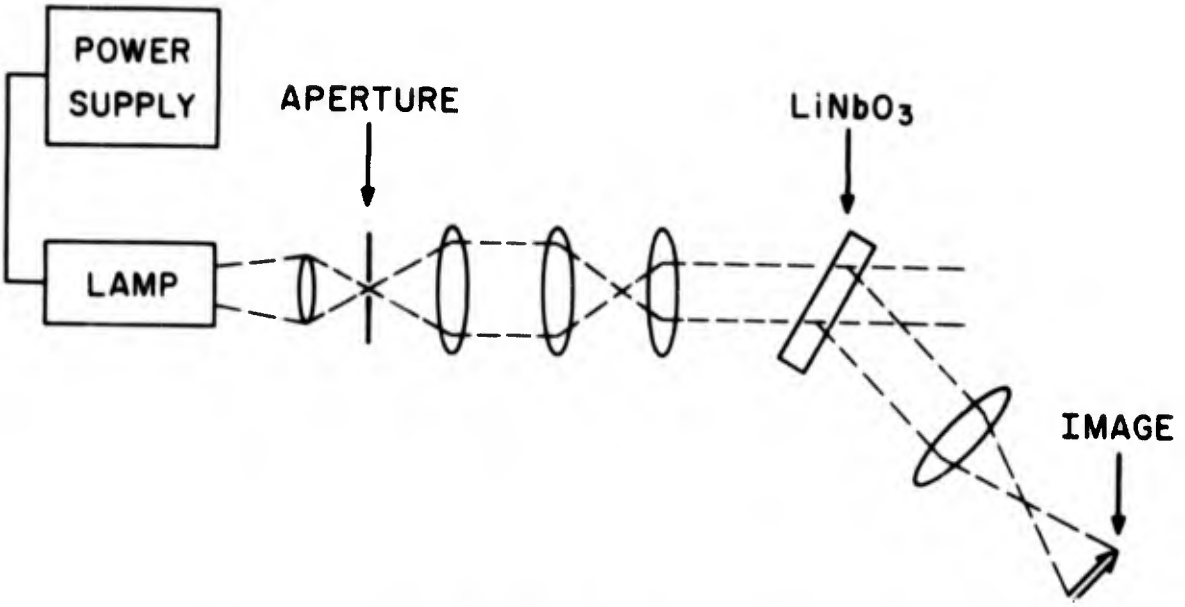

Figure 18. Optical system for incoherent readout.

C. RESULTS

The utility of incoherent readout as a technique for retrieval of holograms stored in a thick medium depends upon the readout efficiency relative to that for coherent readout and the angular selectivity of the medium. We shall discuss here detailed measurements of these properties, which we have made during this period, and a simple model which enables us to understand the results obtained.

The efficiency for incoherent readout of a focused-image hologram was measured with several configurations for collecting light from the xenon arc source. For light polarized parallel to the c-axis of the crystal the optimum efficiency for readout ranged between 10 and 25% of that obtainable with laser light at the wavelength at which the hologram was recorded. An example of this would be a focused-image hologram recorded at 4880 Å with an efficiency of 15%. For incoherent readout the optimum efficiency of the same hologram ranged from 1.5% to 4%. This range of values of the efficiency is due to a variation in the degree of spatial coherence or collimation. The degree of coherence or collimation was varied by changing the size of the aperture in the collection and collimation optics. When the size of the pinhole was decreased from 3000 μm to 250 μm the efficiency for readout increased by more than a factor of two, but the amount of light incident on the storage medium decreased by a factor of 200. Figure 19 shows the efficiency and image brightness as a function of aperture size.

The efficiency for incoherent readout was measured at five different wavelengths (4900 Å to 6328 Å) spanning the visible spectrum, using interference filters with a bandpass varying from 60 Å to 100 Å. The efficiency was found to be essentially constant across this range.

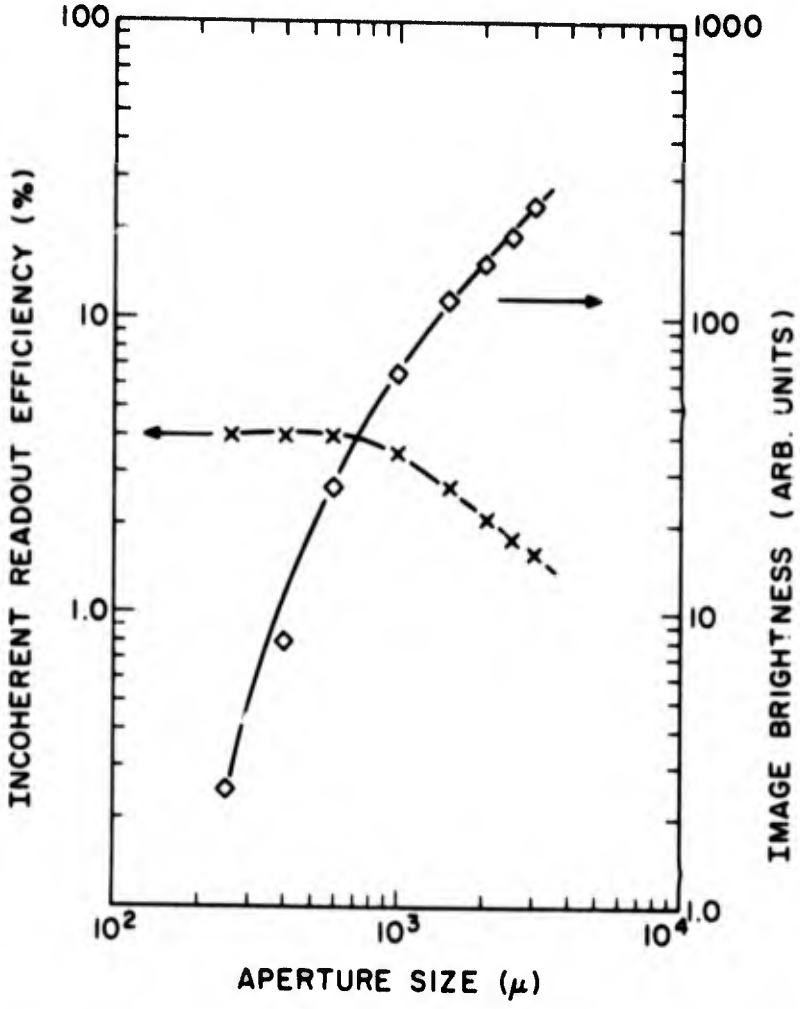

Figure 19. Effect of spatial coherence on incoherent readout efficiency and image brightness for a quasi-focused image hologram.

The angular selectivity for incoherent readout was measured using the light transmitted through interference filters centered at 5460 Å and 5790 Å. The bandpass of these filters was 65 Å at 5460 Å and 70 Å at 5790 Å. The corresponding range of angles over which the hologram could be read out was 66 mrad at 5460 Å (to zero on *both* sides of the *main diffraction* peak). These values are to be compared with a value of 2.75 mrad expected for this thickness for coherent readout at 4880 Å

The principal results of these measurements are, then, that the efficiency for incoherent readout is about 10% of that obtainable for coherent readout and the angular sensitivity is approximately 25 times less using 60-Å to 70-Å bandpass filters. To determine whether these results are optimal and consistent with the known properties of thick-phase holograms we can consider a simple model of the readout process for an incoherent source. The temporal coherence of a light beam is measured as the distance over which the beam

maintains a constant phase as a function of time. The spectral purity of a light source is a direct measure of its temporal coherence, and the coherence length is $\Lambda = \lambda^2/\Delta\lambda$, where $\Delta\lambda$ is the full width at half maximum of the incident light. Since Λ is a measure of the distance over which a light beam maintains a constant phase relation, it is also a measure of the distance over which constructive interference and thus Bragg diffraction can occur. For the 4880-Å line of the Ar^+ laser $\Lambda \sim 5$ cm, and Bragg diffraction can occur in crystals several centimeters thick. For a 65-Å-wide source at 5460 Å $\Lambda = 46$ μm. Thus, in this case, the thickest phase hologram for which Bragg diffraction can occur is of the order of 46 μm. For the xenon arc the diffracted *intensities* from each thickness Λ of the crystal will add since they are incoherent with one another. The total efficiency is

$$\eta_I = N \sin^2 \left(\frac{\pi \Delta n \Lambda}{\lambda \cos \theta/2} \right) \tag{22}$$

where $N = d/\Lambda$ and d is the thickness of the crystal. For the 4880-Å laser line the diffracted *amplitudes* from each thickness Λ will add since they are coherent with one another. In this case, the total efficiency is

$$\eta_c = \sin^2 \left(\frac{\pi \Delta n \Lambda N}{\lambda \cos \theta/2} \right) \tag{23}$$

The relative efficiency of incoherent to coherent readout is

$$\eta = \frac{\eta_I}{\eta_c} = \frac{N \sin^2 \left(\frac{\pi \Delta n \Lambda}{\lambda \cos \theta/2} \right)}{\sin^2 \left(\frac{\pi \Delta n \Lambda N}{\lambda \cos \theta/2} \right)} \tag{24}$$

For $\eta_c \lesssim 15\%$

$$\eta \approx \frac{N \left(\frac{\pi \Delta n \Lambda}{\lambda \cos \theta/2} \right)^2}{N^2 \left(\frac{\pi \Delta n \Lambda}{\lambda \cos \theta/2} \right)^2} = \frac{1}{N} = \frac{\Lambda}{d} \tag{25}$$

For a crystal 0.182 cm thick and a 65-Å bandpass (FWHM) for incoherent light, $\eta = 2.5\%$ which is a factor of $\sim$10 less than the highest measured value.

The angular selectivity for a hologram of thickness Λ is [14]

$$\Delta\theta = \frac{n\lambda}{\Lambda} \frac{\cos \theta'/2}{\cos \theta/2 \sin \theta/2} \tag{26}$$

For $\theta = 30°$, $\Lambda = 46$ μm and $\lambda = 5460$ Å, $\Delta\theta = 122$ mrad which is a factor of two greater than the measured value. Similarly at 5790 Å, $\Delta\theta = 129$ mrad. These values are to be compared with measured values of 66 mrad and 74 mrad, respectively. This model also predicts the observed increase in $\Delta\theta$ with wavelength.

This approximation, which treats the crystal as a stack of thick phase holograms each of which is Λ thick, predicts the reduction in relative efficiency to a factor of ten and the reduction in angular sensitivity to within a factor of two. The discrepancy in each case is in the same direction; i.e., if the effective hologram thickness is 2 Λ, then the angular sensitivity is in good agreement and the relative efficiency is within a factor of five. While the approximations used here are quite clearly crude, the model also leads to the correct result that $\eta \sim 1$ for white light readout of thin-phase holograms. A more detailed calculation may lead to closer agreement with the measurements discussed above.

The most important element is the incoherent readout process is, then, the temporal coherence of the readout beam. Increasing the coherence length will increase both the readout efficiency and the angular selectivity. An increase in the coherence length by narrowing the spectral bandwidth does not lead to a decrease in image brightness, at least up to a point, as a simple calculation shows. The diffracted power is

$$P_I = P_o \eta_I = P_o \Lambda \eta_c / d \tag{27}$$

where P_o is the incident power, and the other symbols are as defined above. If the lamp output spectrum is flat over the wavelength range of interest, then

$$P_o = K \Delta\lambda \tag{28}$$

where K is a constant. The diffracted power becomes

$$P_I = \frac{K \Delta\lambda \Lambda}{d} \eta_c = \frac{K \lambda^2}{d} \eta_c \tag{29}$$

which is independent of the spectral bandwidth. Thus, it would appear that the spectral purity or color saturation can be enhanced as well as the angular selectivity without a concomitant loss of image brightness. There is an upper limit to a useful coherence length which is either the crystal thickness or the onset of destructive interference of light diffracted from different volumes of the phase grating. This latter effect arises from the fact that the Bragg condition cannot be satisfied over a large volume at wavelengths different from that at which the grating was recorded[15]. This effect is quite pronounced when readout is attempted with a different laser line than that at which the hologram is recorded. Such interference effects were not observed here for incoherent readout because of the short coherence length.

D. CONCLUSIONS

From the simple model discussed above it is clear that the coherence length or spectral bandwidth of the source is the dominant factor in the incoherent readout of thick-phase holograms. The efficiency for incoherent readout approaches that for laser readout as the coherence length becomes comparable to the crystal thickness. There are, however, no sources except the high pressure mercury arc at 5460 Å which has an output whose brightness is within several orders of magnitude of that of a laser. Thus, an image brightness comparable to that obtainable with a laser can never be achieved. In addition, if a hologram is recorded at say 4880 Å and read out at 5460 Å with a spectral bandpass $\Delta\lambda \lesssim 5$ Å, the image quality is severely degraded due to interference effects arising from the fact that at 5460 Å the Bragg condition for 4880 Å cannot be satisfied over large areas of the object. If, on the other hand, we choose to use a large bandwidth source, both the efficiency for incoherent readout and the angular selectivity of the medium decrease. This is in contrast to the case for thin holograms where the coherence length is always greater than the hologram thickness, and thus a broad-band source can be used to increase the brightness. There is, however, no angular selectivity for a thin hologram.

In conclusion, the measurements discussed above and the simple model used to interpret them indicate that incoherent readout of thick phase holograms stored in an electro-optic medium is not a viable approach for direct display of information in a moving map display.

VII. ELECTRONIC DISPLAY

The results obtained in Section VI and the relative comparison of direct and indirect displays to be made later in this report show that the only viable format for the display of information in a high light ambient is the use of an electronic display. An electronic display in this context covers a variety of different devices: color kinescope or scanned laser using vidicon pickup, direct projection into a light valve and others. In this program we have concentrated on the application of electronic color-encoding techniques for the storage of color images in thick phase media and the display of the reconstructed image on a color kinescope. In this section, we shall discuss the results obtained in this area.

A. ELECTRONICS

In a previous program[11] a two-frame electronically encoded color transparency was recorded and fixed in a crystal of $LiNbO_3$. This hologram was reconstructed and the separate frames were imaged onto two separate monochrome cameras. The video signals were then decoded and the color image displayed on a commercial color monitor. The use of two cameras led to problems of mechanical alignment and misregistration in addition to the cumbersome setup required.

During the current program the two-camera system was replaced with a Bivicon camera, and a more sophisticated electronic decoding system was constructed[16-18]. The key to the simplification of the display system was the use of the Bivicon camera developed at RCA Laboratories. In this camera two photosensitive targets are contained in the same tube. With this arrangement both targets share the same deflection electronics, and the effect of thermal and mechanical drifts is minimized. The use of this tube also led to considerable simplification in the mechanical setup and alignment procedure since the reconstructed image containing the two frames was simple imaged on the tube face.

B. RECORDING ARRANGEMENT

The primary requirement of the imaging optics in the holographic recording system is that the object transparency be imaged on the Bivicon target with a magnification such that the two frames are centered on the respective targets. In this case, a magnification of 1.38 was required to match the frame separation of 7.6 mm to the target separation of 10.5 mm. A single lens in the recording apparatus was sufficient to provide the required magnification. This system, shown in Fig. 20, had the additional advantages that an imaging lens for the Bivicon was not required, and the coherent noise from imperfections in the system optics was reduced by the elimination of this lens.

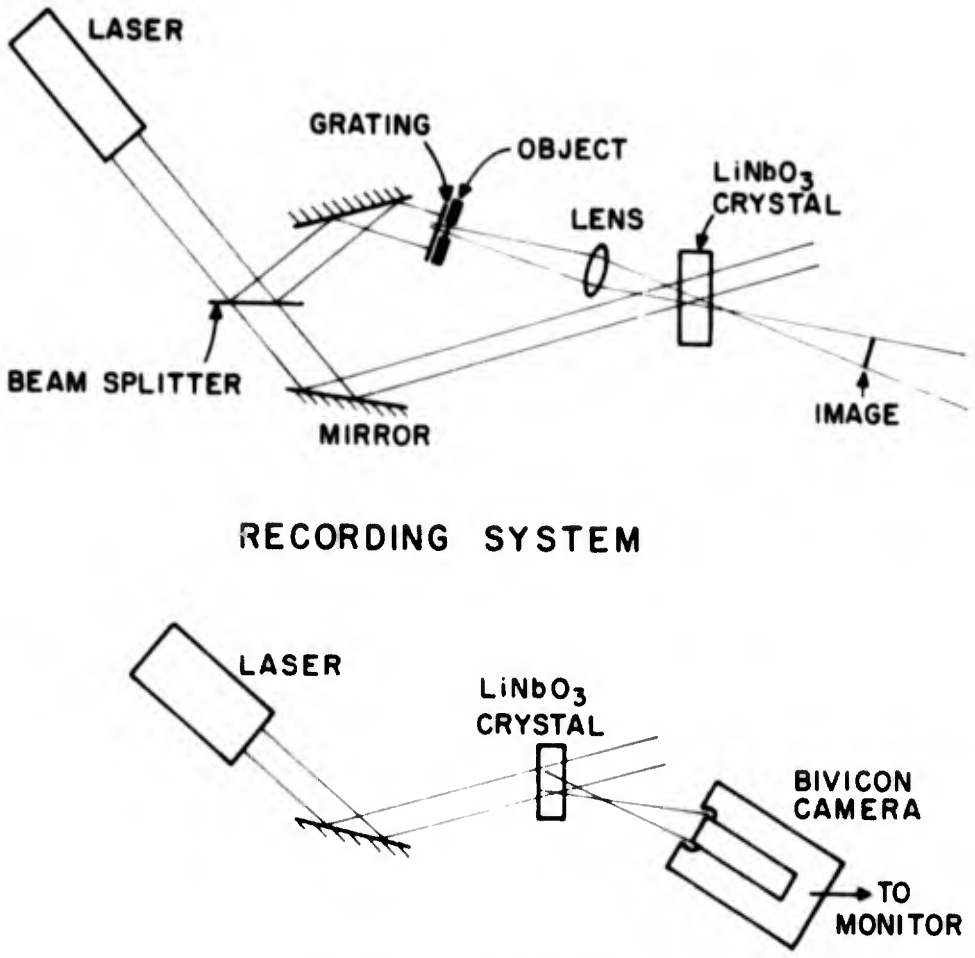

Figure 20. Optical system used for recording and readout of holograms of color-encoded transparencies.

C. REDUNDANCY

Coherent light, when used for the recording and readout of information stored in a hologram, becomes a source of noise in the displayed image. This noise has two components. The first of these is speckle noise which is common to all laser displays. The second is diffraction from imperfections in the recording or readout optics or in the recording medium itself. This noise can be significantly reduced by causing the light which illuminates a particular point in the object plane to travel through the optical system with a number of different paths. The fraction of the light diffracted from a particular point in the object which is intercepted by a defect in the optical system is reduced thus producing an increase in the signal-to-noise of the image.

The technique used to achieve this goal is to illuminate the object with a multiplicity of beams[19]. In the present program, two-dimensional sinusoidal

gratings recorded in photoresist and which produced nine beams of approximately equal intensity were used. In this way, approximately a nine-fold increase in the redundancy of the recorded hologram was obtained.

D. RESULTS

The addition of a two-dimensional phase grating to introduce redundancy into the recording system improved the quality of the color image obtained considerably. Noise from imperfections in the optics was still present indicating that the degree of redundancy required will have to be increased. Examination of the gratings available using direct projection of an encoded transparency indicated that a part of the problem lay in nonuniformities in the grating itself. An effort is now under way to make higher-quality gratings than those at hand.

From the initial results obtained in this program it appeared that the high optical quality of the $LiNbO_3$ crystals used as a storage medium would decrease the redundancy requirements from those required in other systems. The results obtained to date indicate that noise in the optics is the dominant factor in the determination of image quality. The optical quality of the $LiNbO_3$ does enter directly in that optical damage, which accumulates with prolonged readout, becomes a source of noise in the readout hologram and contributes to degradation of the color image. In an effort to reduce the importance of optical damage a narrow band interference filter at the readout wavelength was placed in front of the Bivicon. With this filter in place, an incoherent source such as a tungsten filament can be used to illuminate the crystal uniformly to suppress the buildup of optical damage. The addition of this filter introduced some noise into the image due to imperfections in the filter. This was reduced with the use of the redundancy device and will be further reduced when filters with better optical quality are obtained.

E. CONCLUSIONS

The images obtained from the encoded transparencies were of good quality. The introduction of redundancy through the use of multiple beam illumination of the object led to a considerable improvement in the image quality. It is clear that both in this area and in the quality of the optical syste significant improvements can be made. It is apparent though, that with sufficient effort a display based upon volume storage of color-encoded objects is feasible.

In addition to the experimental work discussed above, a theoretical understanding of the relative importance for volume storage of images of different sources of noise such as intermodulation distortion and crosstalk, as well as coherent scattering of light, is required. In particular, an understanding of the applicability of the theory of suppression of coherent noise with redundancy in thick, as opposed to thin, phase holograms is required. An example in point, which appears to be consistent with our observation of the image quality of high diffraction efficiency holograms, is that intermodulation distortion is suppressed proportional to the hologram thickness[20].

VIII. SYSTEM EVALUATION AND CONCLUSIONS

A volume holographic read-only optical memory has three basic components: the accessing system, the storage medium itself, and the image display device. In this section, we shall evaluate each of these areas in light of what has been learned in this program. In each case the future direction that this program should take will be discussed.

A. RETRIEVAL TECHNIQUES

One of the primary advantages of a volume holographic read-only memory is its potentiality in a fast, random-access mode. In Section V of this report galvanometers and stepping motors were evaluated while acousto-optic deflectors were evaluated in an earlier program. Based upon this work a comparison of capabilities can be made and tradeoffs in the choice of a particular device can be understood.

The galvanometer is a simple, low-cost device with high angular resolution. It is, however, sensitive to both thermal and mechanical perturbations and has an inherent hysteresis problem. The galvanometer used here (General Scanning Model G-330) has a temperature sensitivity of 0.02%/°C. Changes on the order of 10°C will change the calibration of the device to the extent that hologram addressing would be impossible without a coded addressing scheme on individual holograms. In a laboratory environment the galvanometer can perform satisfactorily with crystals less than 0.5 cm thick but their mechanical stability presents a serious problem both in general as well as in extreme conditions. The hysteresis effect noted in Section V can be overcome in accessing applications where servo loops are not required, but this effect has presented difficulties in our preliminary studies of servo techniques.

Work at RCA Laboratories and elsewhere has led to the development of the paratellurite (TeO_2) acousto-optic deflector. Up to 500 fully resolved spots with 90% diffraction efficiency have been obtained using a current RCA TeO_2 deflector[21]. This device operates at a 67-MHz center frequency with a 65-MHz bandpass and requires 40 to 60 mW of rf power. The access time obtained for the 500-spot deflector is 20 μsec. The reduction of an order of magnitude in the rf power requirements, combined with the mechanical stability and smaller temperature sensitivity of the TeO_2 deflector, makes this device appear to be the better choice at this time as opposed to mechanical devices such as a galvanometer.

The electrical system discussed in Section V-C provided sufficient accuracy for the requirements of this program. However, an increase in scale to a retrieval system capacity of the order of 1,000 holograms will require more sophisticated techniques than those used here, particularly in those cases where an acousto-optic deflector is used.

B. STORAGE MEDIUM

The development of improved fixing techniques for the most sensitive Fe-doped $LiNbO_3$ and the application of these techniques constitute a significant step toward the development of a volume holographic storage system. The write-erase asymmetry present at the fixing temperature is sufficient for the storage of a large number of holograms as discussed in Section III. Since the write-while-hot technique permits the recording of high diffraction efficiency holograms without beam coupling effects and significant amounts of optical damage, the original projection of 1,000 holograms with a diffraction efficiency greater than 0.01% should be obtainable. The recording of 100 holograms, each with a diffraction efficiency greater than 1% as obtained during this program, is consistent with that projection.

In addition to the still somewhat primitive recording techniques, two other areas in which material improvements or new materials would have a significant impact on this program are (a) an increase in the writing sensitivity of the storage medium and (b) a reduction in the optical damage during prolonged readout.

Increases in the writing sensitivity could come from either of two sources: improvements in the Fe-doped $LiNbO_3$ or development of new materials with sensitivity greater than that of $LiNbO_3$. Preliminary investigations in this area have begun under a materials research program sponsored by the Naval Air Systems Command[7].

Photochromic $LiNbO_3$[4,5] offers one of the most interesting possibilities for the reduction of optical damage during readout. After hologram recording and fixing electrons trapped at Fe^{3+} sites are photo-ionized and trapped at other sites in the crystal which do not absorb light at 4880 Å. Since the readout light is not absorbed, optical damage is suppressed. Until now, however, these materials have not been as sensitive and do not fix as well as the best singly-doped-crystals. An additional advantage of the photochromic materials is that since the absorption is reduced at the readout wavelength the usable diffraction efficiency is increased.

C. DISPLAY FORMAT

From the point of view of system configuration and ultimate storage capacity, the most important consideration is the final form of display. The two alternatives are (a) direct display, where the light diffracted by the medium is used to reconstruct the viewing images without any buffering, and (b) indirect display, where the image is picked up by an electronic device that controls the final display. The major differences are in the diffraction efficiency required from the medium and in the method of color encoding that can be used.

1. Direct Display

There are two approaches to the direct display of images stored as thick phase holograms. They depend on whether a laser or an incoherent source is

used to reconstruct the image and project it onto an appropriate viewing screen. In this section, we shall consider the question of whether either of these approaches is a viable alternative for the display of maps.

Use of a laser source allows one to exploit the large angular packing density of thick phase gratings and the high resolution capabilities of the electro-optic medium. There are several difficulties with the use of a laser. The first is that to produce a direct color image two lasers or a mixed-gas laser must be used. The use of two large lasers is uneconomical. The use of a mixed-gas system is questionable because of difficulties with broadband mirror coatings. A second difficulty is that the writing sensitivity for the red primary color is poor for all known materials. A third problem with direct readout, which is also common to a system using incoherent readout, is that the readout efficiency per stored hologram decreases as the number of holograms stored in a given volume increases. At the present time 100 holograms can be stored and fixed with an efficiency greater than 1%, while for 1000 holograms the corresponding efficiency would be of the order of 0.01%. These efficiencies are marginal for a direct display of suitable brightness, even at the 100-hologram level.

The use of an incoherent source for the readout of thick-phase holograms, which was discussed in Section VI of this report, is an attractive alternative to a laser source since it is simpler and more economical, meets the overall system requirements on power consumption, and provides the three primary colors from a single source. The measurements and the simple model for incoherent readout discussed above showed that there were several tradeoffs in the use of an incoherent source. The primary result was that the optimum performance was obtained for a source whose coherence length was of the order of the crystal thickness. For a 0.2-cm-thick crystal this length corresponds to a source bandwidth of 1.5 Å at 5500 Å. Thus, we must seek an incoherent source with brightness comparable to that of a laser over a bandwidth of several angstroms. There are no sources other than the Hg line at 5460 Å which possess a brightness comparable to that found in laser sources.

For a 1000-W Xe arc the energy collected by a lens which subtends a solid angle of 0.32 steradian and which focusses the collected light through a 1/8-in.-diam. pinhole (the system used in this work) is approximately 0.16 mW/Å in the visible range. For a 1000-W Hg or Hg-Xe arc the output at 5460 Å is approximately 5 mW/Å. Small Ar^+ helium-neon or helium-cadmium lasers can easily produce outputs larger than these values at the corresponding wavelengths.

An estimate of the power incident on the viewing screen of a direct display can be made from previous work[22]. We estimate that 10-mW incident power is required to provide a usable image on a 6-in.-diameter screen. The efficiency of the optical system (exclusive of the hologram) was ~63%. If we assume that this is a reasonable value for system efficiency, then for a 1% efficient hologram, the required optical power input to the system is 1.57 W. This value is far in excess of the capability of incoherent sources discussed above. The size of the laser required to produce 1.57 W is also in excess of the overall system specification for electrical power consumption.

Thus, it is clear that, with multiple storage, a direct display of maps in $LiNbO_3$ is not feasible because of overall power consumption and because of lack of sufficient image brightness.

2. Electronic Display

In systems where direct display cannot satisfy overall system requirements an electronic display may provide an adequate solution. This approach includes an electronic pickup, such as a vidicon, and a buffer which decodes the pickup and provides for proper visual display. Normally, such a system would include a kinescope for final viewing but is not limited to this approach.

The advantages of electronic display are several. Among the most important are:

- Low diffraction efficiency holograms may be used because of the high sensitivity of the vidicon pickup. This would result in much increased storage capacity.
- Color display can be produced with a variety of formats (one, two, or three frames) and require a single wavelength for recording and readout.
- The sensitivity of the electro-optic medium need be high only at one wavelength and not over a broad range of wavelengths.
- Low-power lasers can be used, thus reducing system cost and complexity.
- Increased flexibility in the display format and in the addition of read-time information to the visual display.
- Simpler annotation and dynamic symbology.

The disadvantages of this approach are:

- The resolution capabilities of the present electronic display based on color kinescope are the order of 350 lines with a potential increase of up to a factor of two in resolution.
- Increased complexity and possible cost in terms of the added electronics.

The results obtained to date with the two-frame encoding technique show that this approach should yield, with further effort, a color display of the required quality. The high optical quality of $LiNbO_3$ crystals appears to reduce the redundancy required for this application as compared with other storage materials such as Photoresist.

The limited resolution of kinescope displays negates, as noted above, the high resolution storage capability of $LiNbO_3$. Systems such as a scanned laser coupled with a high resolution vidicon or a light valve are alternative formats which will have to be considered for higher-resolution displays.

D. IMAGE QUALITY

The object transparencies used in this program were recorded in high contrast emulsions on glass plates in a 35-mm format or on Kodak EBR special 16-mm film. The images reconstructed from holograms recorded with the 35-mm glass slides were cosmetically of better quality because of the format size which reduces the sensitivity to imperfections in the emulsion and dust on the emulsion as well as to the higher object contrast ratio obtainable with the glass plates. These results indicate that redundancy should be added to the recording system even in the case of monochrome images to compensate for imperfections in both the object and the recording optics. This is true whether a vidicon pickup or direct display of the readout images is used.

The ultimate limitation on the storage capacity in the range between 100 and 1000 holograms will be determined by the required signal-to-noise ratio. In addition to the coherent noise from imperfections, additional sources of noise in the readout image peculiar to volume storage must be considered. Ramberg[12] has considered two sources of such noise: (a) linear crosstalk between images and (b) fluctuations in the intensity in the reconstructed image arising from the statistical distribution of the trapped charge which produces the phase grating. Neither of these noise sources was explicitly investigated during the current program. The problem of linear crosstalk did arise in this program when an effort was made to record more than a few holograms in the same volume as was shown in Fig. 10. A practical criterion for the angular spacing of four to five times the zero-to-zero angular width of the main diffraction peak was used in this work. The acceptable level of crosstalk in an image will derermine the angular spacing used in a practical system and, when taken together with the statistical effect, will determine the ultimate capacity of a volume storage medium. The optimization of the storage capacity and the signal-to-noise ratio thus constitutes one of the most important tasks remaining in the development of the volume holographic storage system.

E. CONCLUSIONS

The evaluation of the various components of a volume holographic storage system to be used as a moving map display or in other read-only memory applications emphasizes the fact that while major progress has been made during this program, a number of problems remain to be solved. The recording and fixing of 100 holograms in Fe-doped $LiNbO_3$ represent a significant achievement of this program and augurs well for the attainment of our ultimate goal of 500 to 1000 holograms stored and fixed. Detailed analysis and measurement of image noise sources are required, however, since these effects will ultimately limit the capacity of the storage medium. These measurements are of particular importance since they bear directly on the practicality of the proposed system. An estimate of the limits imposed should be obtainable in a concentrated effort with the materials at hand. The influence of material parameters on noise sources will, when properly interpreted, serve as a guide for further materials development.

The importance of increased understanding of the material properties was clearly demonstrated by the impact of the development of the write-while-

hot technique on our success in recording and fixing 100 holograms. Future efforts to increase the write-erase asymmetry and to reduce the effects of optical damage during readout will be of great importance to an effort to increase the image quality.

The conclusions drawn from the results obtained in this program indicate that the next steps required are fourfold:

- Scaling up of the present system from 100 to the range of 500 to 1000 holograms stored and fixed.
- Measurement and analysis of the noise sources in a volume holographic storage system.
- Continued effort to improve the material performance.
- Optimum retrieval system for 1000 holograms.

APPENDIX A

EXPOSURES FOR MULTIPLE STORAGE

To fully utlize the multiple storage capacity of Fe-doped $LiNbO_3$, one must take into account the optical erasure effect discussed in Section III. The sequential exposures should be chosen such that at the completion of the storage process, all holograms have approximately the same diffraction efficiency. In this appendix, we derive a relationship for the required exposures, and use this relationship to determine the limitation of the erasure problem on the diffraction efficiency.

The basic requirement for equal efficiencies is shown in Fig. 21. The diffraction efficiency is shown as a function of exposure for a number of separate writing operations. At the end of each operation, the crystal is rotated slightly, and then another hologram is recorded. The dotted line shows the erasure that occurs during storage. Here, the exposures are chosen so that the erasure is perfectly compensated. Consider the second exposure. It is stopped when the storage curve of the second hologram intersects the erasure curve of the first hologram. As a result, both holograms have the same diffraction efficiency and erase along the same curve as the third hologram is recorded. By repeating this procedure, any number of equal-efficiency holograms can be recorded.

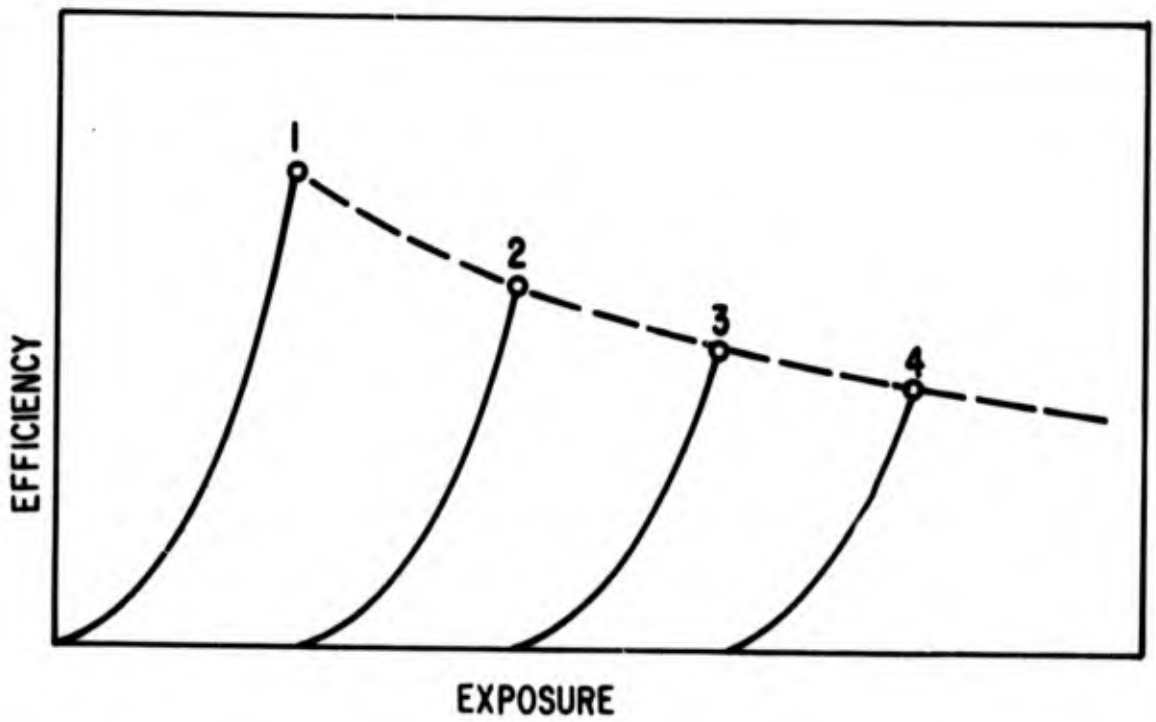

Figure 21. Storage (solid lines) and erasure (dotted line) during a multiple recording process that perfectly compensates for erasure.

In practice, the required exposures cannot be experimentally determined. The storage is done at elevated temperatures at which the holograms are latent, i.e., they cannot be observed. The best approach is to calculate the exposures from the well-established writing and erasing behavior of holograms in electro-optic crystals. In these materials, the appropriate functions are given by

$$\text{write:} \quad \eta \sim \mathcal{E}^2 \tag{30}$$

$$\text{erase:} \quad \eta \sim \exp\,[-2\mathcal{E}/\mathcal{E}_e] \tag{31}$$

where η is the diffraction efficiency, $\mathcal{E}$ is the exposure time, and $\mathcal{E}_e$ is the time required to decrease the efficiency by e^2 ($\sim$0.75). If the nth hologram is to have the same diffraction efficiency as the previous one, we must have

$$\eta_n = \eta_{n-1} \exp\,[-2\mathcal{E}_n/\mathcal{E}_e] \tag{32}$$

where $\mathcal{E}_n$ is the exposure for the nth hologram. Since

$$\frac{\eta_n}{\eta_{n-1}} = \left(\frac{\mathcal{E}_n}{\mathcal{E}_{n-1}}\right)^2 \tag{33}$$

we have for perfect compensation of erasure

$$\frac{t_n}{t_{n-1}} = \exp\,(-\mathcal{E}_n/\mathcal{E}_e) \tag{34}$$

Equation (35 cannot be solved directly in a closed form, but can be simplified by assuming that the storage time of any of the holograms is much smaller than that required for erasure, i. e.,

$$\mathcal{E}_n \ll \mathcal{E}_e \tag{35}$$

This type of write/erase asymmetry is highly desirable for increasing the storage capacity and can be easily achieved. Making this assumption, Eq. (5) becomes

$$\frac{\mathcal{E}_n}{\mathcal{E}_{n-1}} = 1 - \frac{\mathcal{E}_n}{\mathcal{E}_e} \tag{36}$$

or

$$1/\mathcal{E}_n - 1/\mathcal{E}_{n-1} = 1/\mathcal{E}_e \tag{37}$$

By iteration this gives

$$1/\mathcal{E}_n - 1/\mathcal{E}_1 = (n - 1)\mathcal{E}_e \tag{38}$$

or finally

$$\mathcal{E}_n = \frac{\mathcal{E}_e}{(n - 1) + \mathcal{E}_e/\mathcal{E}_1} \tag{39}$$

where $\mathcal{E}_1$ and $\mathcal{E}_n$ are the exposures of the 1st and nth holograms, respectively. This gives the successive exposures needed to obtain equal diffraction efficiency for all n holograms. Note that, as expected, the exposures must become progressively smaller.

We can calculate the diffraction efficiency of the n holograms with Eqs. (39) and (30). These yield

$$\eta_n = \eta_1 [1 + (n - 1)/\beta_1]^{-2} \tag{40}$$

where

$$\beta_1 = \mathcal{E}_e/\mathcal{E}_1 \tag{41}$$

The total exposure required to obtain these holograms is derived by summing Eq. (39):

$$\mathcal{E}_{total} = \sum_{n'=1}^{n} \mathcal{E}_{n'} = \sum_{n'=1}^{n} \frac{\mathcal{E}_e}{(n' - 1) + \beta} \tag{42}$$

For a β of a much greater than unity ($\geq$ 10) and for an even larger value of n, this can be approximated by integrating Eq. (42) to get

$$\mathcal{E}_{total} = \mathcal{E}_e \ln \frac{n}{\beta} \tag{43}$$

Using the same approximation, we derive the diffraction efficiency of the n holograms from Eq. (40)

$$\eta_n = \frac{\eta_1 (\mathcal{E}_e/\mathcal{E}_1)^2}{n^2} \tag{44}$$

REFERENCES

1. F. S. Chen, J. T. LaMacchia, and D. B. Fraser, Appl. Phys. Letters 13, 223 (1968).
2. J. J. Amodei, W. Phillips, and D. L. Staebler, Appl. Optics 11, 390 (1972).
3. W. Phillips, J. J. Amodei, and D. L. Staebler, RCA Review 33, 94 (1972).
4. D. L. Staebler, W. Phillips, and B. W. Faughnan, Final Report, Contract N00019-72-C-0147, March 1973.
5. D. L. Staebler and W. Phillips, First Quarterly Report, Contract N00019-73-C-0273, April 1973.
6. J. J. Amodei and D. L. Staebler, Appl. Phys. Letters 18, 540 (1971).
7. D. L. Staebler and J. J. Amodei, Ferroelectrics 3, 107 (1972).
8. D. L. Staebler and J. J. Amodei, J. Appl. Phys. 43, 1042 (1972).
9. H. Kogelnik, Bell System Tech J. 48, 2909 (1969).
10. D. L. Staebler, W. J. Burke, and J. J. Amodei, Post-Deadline Paper, Conference on Laser Engineering and Applications, Washington, D.C., May 1973.
11. J. J. Amodei, W. J. Burke, and D. L. Staebler, Final Report, Contract N62269-71-C-0533, July 1972.
12. E. G. Ramberg, RCA Review 33, 5 (1972).
13. S. C. Abrahams, H. J. Levenstein, and J. M. Reddy, J. Phys. Chem. Solids 27, 1019 (1966).
14. H. M. Smith, *Principles of Holography*, (Wiley-Interscience, New York, 1969) p. 69.
15. E. G. Ramberg, RCA Review 27, 467 (1966).
16. R. L. Spaulding et al., Proc. IEEE 60, 1236 (1972).
17. R. L. Spaulding, S. A. Ochs, and E. Luedicke, RCA Review 34, 121 (1973).
18. R. E. Flory, RCA Review 34, 134 (1973).
19. A. H. Firester et al., RCA Review 33, 131 (1972).
20. R. Baugh, PhD. Thesis, Stamford University (1969).
21. I. Gorog, J. Knox, P. V. Goedertier, and I. Shidlovsky, RCA Review 33, 667 (1972).
22. G. T. Burton, B. R. Clay, R. F. Croce, and D. A. Gore, *Laser-Hologram Multicolor Moving Map Display System*, Final Report, Contract N62269-70-C-0080.